Data Analysis for Predicting Instabilities in Power Systems

A THESIS

submitted by

Aryan Ritwajeet Jha

2020EEY7525

under the guidance of
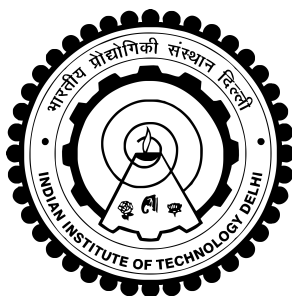
Prof. Nilanjan Senroy

for the award of the degree

of

Master Of Science

(by Research)

Department Of Electrical Engineering

INDIAN INSTITUTE OF TECHNOLOGY DELHI

August 2022

Chapters for the Thesis

Chapter 1

Introduction

Unlike transient faults in a power grid which can generally be attributed to a sudden but tangible anomaly (corrective outcomes of protection mechanisms, sudden failure of a generator or transformer, line faults), certain indicators of proximity to instabilities may remain undetected until they accumulate over time to manifest as a major upset to the grid [1] and/or make the grid less robust/more susceptible to collapses [2]. The causes of these disturbances is often an accruing of stochastic perturbations in the state variables of the grids when it is already stressed by an increased power demand [3]. The accrual of stochastic perturbations in turn can be caused due to various physical phenomena, including measurement errors, distributed renewable generation fluctuations [4], sudden gaps in power demand and supply due to power trading [2], strict operational frequency deadbands [5, 6], etc.

While modeling every significant possible source of stochastic disturbance can be difficult or perhaps even outright impossible, at least their detection can be made through model free data-driven statistical analysis, enabling early detection of grid stability problems for a timely course-corrective action [2, 7, 8].

Bifurcation Theory [3, 9–11] helps explain the erratic functioning of stressed dynamical systems such as the power grid, and the theory of Critical Slowing Down [12] lists tangible quantitative analysis tools which can help us detect an impending 'bifurcation' (blackout) in the power grid.

In this thesis, firstly various real-world grid frequency time series archives were investigated on their robustness against minor disturbances and any kind of long-standing stability problems in them, through the use of bulk distribution probability density functions and autocorrelation decay plots. This analysis is referred to as Offline/Postmortem analysis as the entire span of input data used has already been sampled before the analysis for a long period (several months or years). The chapter concludes with how different grids have varying levels of susceptibility to instabilities based on their size and their inherent dynamics as

well as control and operation mechanisms.

Next, the effectiveness of two statistical parameters computed in real-time listed out as per the theory of Critical Slowing Down, namely Autocorrelation and Variance as Early Warning Sign Indicators of an approaching bifurcation in a power grid. For statistically testing for the increase in autocorrelation and variance of the time-series, a new kind of statistical parameter, namely the Modified Kendall's Tau Correlation Coefficient was introduced, to accommodate for the confidence margins (p-values) associated with the computed correlation coefficients. This analysis has been labeled as the Online/Real-time analysis as the input data here is only in instantaneously available from a stream of data, such as PMU data. It was found that both Fixed Lag Autocorrelation and Variance of the bus voltages serve as reliable early warning signs of indicators to instabilities in power grids. Through the Modified Kendall's Tau Correlation Coefficients, it was visually observed how different buses may be more or less susceptible to a uniform grid-level stress (in the form of a steadily increasing power demand).

The rest of the thesis is as below: Chapter 2: Literature Review and Objectives provides and briefly explains the relevant work performed by the scientific community on predicting early warning signs for instability indicators, followed by how the work done in this thesis provides original contributions to the existing body of literature.

Chapter 3: Theory provides the mathematical foundation required for justifying the Offline Analysis in Chapter 4 and Online Analysis in Chapter 5.

Chapter 4: Offline Analysis provides two kinds of methods of statistically analyzing the bulk distribution of a state variable (grid frequency) of the grid and how meaningful inferences could be made from them. This topic is also called as the Post-mortem analysis because the analysis is performed on data acquired over a long duration of operation of various real-world grids.

Chapter 5: Online Analysis showcases a simulation which uses all of the concepts described in the Theory section in order to test an algorithm for detect early warning signs for indicators to instability. This topic is also called as real-time analysis as the methods described in the chapter are supposed to be done over a real-time stream of data, such as data obtained from a PMU.

Chapter 6 and Chapter 7 are for Conclusions and Future Work respectively.

Chapter 2

Literature Review and Objectives

For offline analysis of the grids, archived frequency time-series data of several real-world grids was downloaded from these websites and/or papers: [13–21]. Schafer et al's paper [2] was referred to for the analysis of these grids. Their paper analyzes how almost all grids show a significant level of deviation from the commonly used assumption that power demand fluctuations follow the Ornstein-Uhlenbeck's Process in which the state variable follows the Gaussian distribution around a nominal mean and a bounded standard deviation. They also explain some of the causes of detected instabilities for various power grids, including measurement errors and energy trading fluctuations.

Most of the recent literature analyzing the effects of Critical Slowing Down on various dynamical systems including but not limited to: power grids, ecological population dynamics, predator-prey ecosystems, prediction of epileptic seizures in patients, climate systems, financial markets, prediction of conversion of vegetation area into deserts, and so on, credit the review made by Scheffer et al in [12]. The paper lists out systems in which Critical Slowing Down has been observed and provides accessible mathematical explanations behind its working, such as why is there an increase of autocorrelation and variance of state variables of real-world physical processes as the system approaches a 'critical bifurcation'. The mathematical term has also been called appropriately as 'critical transition' or 'tipping point' by the author of [22], whose paper explains various normal forms of bifurcations (Fold, Hopf, Saddle Node, Transcritical, Pitchfork) via the concept of fast-slow stochastic systems. For developing a working understanding of bifurcation theory, university lecture notes by [9] and books [10, 11] were utilized.

For real-time/online analysis, authors in [8] have utilized PSAT [23] to simulate a steadily stressed power grid and have demonstrated that the computation of autocorrelation of detrended bus voltages and the computation of variance of detrended line currents can function as reliable Early Warning Signs of increasing instability. The detrending is required in order

to filter any measurement error from the data, which may skew the computed statistical parameters towards bogus values. Adeen et al's paper [4] simulated several Stochastic Differential Equations based on the Ornstein-Uhlenbeck's Process with different values of α (autocorrelation coefficient) and analyzed their Fourier Spectrums to conclude that an increased autocorrelation does in fact lead to a greater amplitude of fluctuations in the state variables of the grid and therefore a higher risk of instability in a power system. Authors in [7] tested various power grids which were driven towards bifurcation and demonstrated that an increase of autocorrelation and variance values of bus voltages (tested in simulation) and grid frequency (tested on the time-series data measured at the Bonneville Power Administration minutes before the blackout of 10 August 1996) can reliably predict the impending bifurcation early enough for mitigating actions to be taken by the grid operator.

For simulation implementations in PSSE 34.3, the community run website run by Jervis Whitley [24] was very helpful.

This thesis aims to highlight how statistical analysis can help predict/observe/detect indicators to instabilities in power grids through both offline and online studies while making the least number of assumptions about the grid models themselves due to its data-driven approach. Statistical analysis can detect both lingering instability causing agents in the grids through Offline/Postmortem Analysis as well as predict any impending blackout/'bifurcation' in the grid through Online/Real-time Analysis. Typical power grid state variables such as Bus Voltages, Line Currents/MVAs and Grid Frequencies obtainable from a stream of PMU data may be used as inputs for such data-driven analysis. Tools used for Offline/Postmortem Analysis are visual inspection of bulk-distribution PDFs and estimating grid damping constants from autocorrelation decay curves. Tools used for Online/Real-time Analysis involve computing fixed-lag autocorrelation and variance of the filtered detrended fluctuations.

All simulations were done in Siemens PSSE 34.3 in conjunction with Python 2.7 (for writing automation scripts). All data analysis was conducted in MATLAB 2022a. A working implementation for anyone interested may be downloaded via [Simulation, Offline Analysis, Online Analysis]

Chapter 3

Theory

Detrended Fluctuation Analysis: A method of analyzing real-world time series for self-affinity, i.e. how correlated a signal's future value is to it's past values. Say, $x(t)$ is a signal from a natural process, then in order to detrend it, it can first be passed via a low-pass filter `LPF` to obtain $\texttt{LPF}(x(t))$ and the resultant signal be subtracted from the original in order to obtain the detrended version of the natural process signal $\tilde{x}(t)$ or $d(x(t))$:

$$\tilde{x}(t) \texttt{ or } d(x(t)) = x(t) - \texttt{LPF}(x(t)) \tag{1}$$

Autocorrelation function: A statistical measure of the correlation of a state variable with a time-lagged version of itself.

$$c(x(t), \tau) = \int_{-\infty}^{\infty} x(t)x(t+\tau)dt \tag{2}$$

In terms of discrete time functions, autocorrelation may be expressed as:

$$c(x[n], \tau) = \sum_{-\infty}^{\infty} x[n]x[n+\tau] \tag{3}$$

It may be noted that the autocorrelation function of any time-varying variable has two degrees of freedom, the first being continuous time t (or instance n for discrete time functions) and the second parameter being the lag τ, i.e. the time duration by which the time-varying variable is displaced/lagged against itself for performing the autocorrelation.

Since in this thesis the function is used in two ways where only one of the parameters is varying (with the other being kept constant) each time, two variations of the autocorrelation function with individual names are specified here:

Fixed Time Autocorrelation: Autocorrelation function computed over a snapshot of

a time-varying variable over a fixed time window. The usage of Fixed Time Autocorrelation can be seen in the Offline Analysis chapter (Chapter 4) of this thesis.

$$c(\tau) = \frac{\sum_{1}^{W_{total}-1} x[n]x[n+\tau]}{\sum_{1}^{W_{total}-1} x[n]^2} \tag{4}$$

In this thesis, the window length W_{total} mostly ranges from months to years, with the exception of a few grids, where it can be for just a few days.

Fixed Time Autocorrelation $c(\tau)$ of any detrended physical/natural signal $\tilde{x}(t)$ or $d(x(t))$, should decrease exponentially as the time-lag τ is increased [2]. The decrement of Fixed Time Autocorrelation with respect to the lag τ is intuitive as it makes sense for a state variable's value to be more correlated with its value a few earlier or later ago than its value thirty minutes earlier or later.

Fixed Lag Autocorrelation: Autocorrelation function computed over a window running over a continuously generated stream of data in which the value of the lag τ is fixed. The usage of Fixed Lag Autocorrelation can be seen in the Online Analysis chapter (Chapter 5) of this thesis.

$$c(t)|_{\tau=\tau_{fixed}} = \frac{\sum_{i}^{i+W-1} x[n]x[n+\tau_{fixed}]}{\sum_{i}^{i+W-1} x[n]^2} \tag{5}$$

In this thesis, the window length W represents the number of consecutive discrete-time instances equivalent to $T = 15$ seconds. The value of τ used is the number of consecutive discrete-time instances equivalent to $\tau_{fixed} = 1$ second. More details in Chapter 5 of this thesis.

Variance: Degree of overall deviation/fluctuation in the values of a data.

$$\sigma^2(x) = E(x^2) - (E(x))^2 \tag{6}$$

where,

$$E(x) = \frac{1}{W} \sum_{i}^{i+W-1} x[n] \tag{7}$$

Bifurcation Theory: The concepts Bifurcations and Critical Bifurcations were used

to explain why a small yet steady change in the parameters of a dynamical system (such as the power grid) can remain inconspicuous only to, upon reaching a 'tipping' point or 'Critical Transition', manifest as a sudden major upset to the 'motion' of the dynamical system. The terms Bifurcations and Critical Bifurcations were used almost interchangeably, although technically only Critical Bifurcations are significant enough to alter the dynamics of a system from stable to unstable. Any dynamical system can be expressed as a set of differential algebraic equations. The Figures 1 and 2 demonstrate this phenomena in a particular variation, the Pitchfork bifurcation.
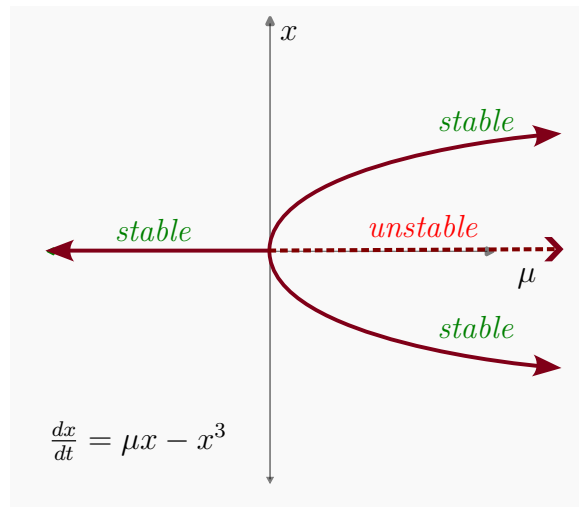
Figure 1: Bifurcation diagram for the normal form of the Supercritical Pitchfork Bifurcation $\frac{dx}{dt} = \mu x - x^3$.
For $\mu \leq 0$, the only stable equilibrium solution for the dynamical system (or fixed point) is $x = 0$. Upon reaching the critical 'tipping' point $\mu = 0$, $x = 0$ no longer remains a stable equilibrium path for the dynamical system and instead two different stable paths emerge: $x = \sqrt{+\mu}$ and $x = -\sqrt{\mu}$. Such a critical point, in which one stable path bifurcates into at least two distinct paths (which may or may not be stable) is called a bifurcation point and the phenomenon is known as 'Critical Bifurcation'.

Critical Slowing Down: The theory of Critical Slowing Down applies on dynamical systems on the verge of 'tipping' or 'bifurcation' and how they show warning signs before breaking down or descending into instability. These warning signs such as an 'increased time to settle', 'increased autocorrelation and variance of fluctuations', etc. [12] can be statistically analyzed to predict the onset of such a bifurcation for a given system.

Why do Autocorrelation and Variance increase with Critical Slowing Down?:
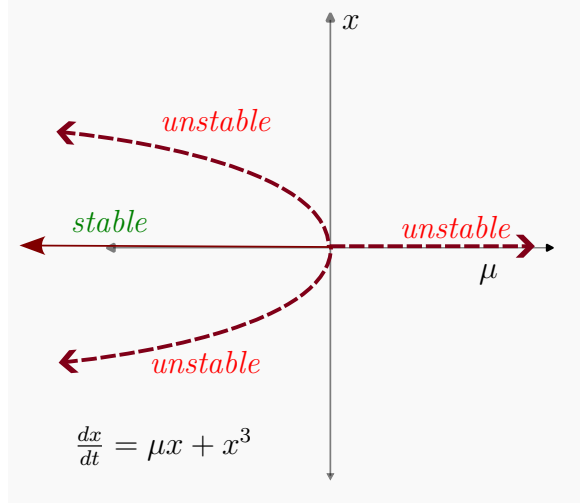
The question may be divided into two parts:

7

Figure 2: Bifurcation diagram for the normal form of the Subcritical Pitchfork Bifurcation $\frac{dx}{dt} = \mu x + x^3$.

For $\mu \leq 0$, the only stable equilibrium solution (or fixed point) for the dynamical system is $x = 0$. Upon reaching the critical 'tipping' point $\mu = 0$, three different equilibrium solutions (or fixed points) emerge: $x = 0$, $x = \sqrt{+\mu}$ and $x = -\sqrt{\mu}$, none of which are stable. Here too, $\mu = 0$ is a bifurcation point.

1. How does the autocorrelation of the perturbations of a system's state variables increase when the system is undergoing Critical Slowing Down?

2. For a system with increasing autocorrelation of the perturbations its state variables, how does the variance of the perturbations also increase?

As an answer to the first question, we may consider the example given in [12]:

Let a dynamical system be represented by the differential function

$$\frac{dx}{dt} = k(x - x_1)(x - x_2) \tag{8}$$

where k is a positive coefficient, x_1 and x_2 are parameters, possibly as result of inherent dynamics of the system infrastructure or an intentional control mechanism (in which case, they are also known as control parameters).

Let x_1 be the stable equilibrium point (or stable fixed point) and x_2 be the unstable equilibrium point (unstable fixed point). This implies that $x_1 < x_2$ (one may easily prove this by taking the second derivatives of Equation 8 and checking for its sign at the fixed points).

Now if the system were to be perturbed at its stable fixed point x_1 by a small disturbance

of Δx, the perturbed dynamical system could be expressed by a slight variation of Equation 8:

$$\frac{d(x_1 + \Delta x)}{dt} = k(x_1 + \Delta x - x_1)(x_1 + \Delta x - x_2) \tag{9}$$

or,

$$\frac{d(x_1)}{dt} + \frac{d(\Delta x)}{dt} = k(\Delta x)(\Delta x + x_1 - x_2) \tag{10}$$

or,

$$\left.\frac{d(\Delta x)}{dt}\right|_{x_1} = k\left\{(x_1 - x_2)\Delta x + (\Delta x)^2\right\} \tag{11}$$

Ignoring the second order terms:

$$\left.\frac{d(\Delta x)}{dt}\right|_{x_1} = k(x_1 - x_2)\Delta x \tag{12}$$

Since the perturbation Δx is independent of the parameters x_1 and x_2, the above equation may be rewritten by replacing $k(x_1 - x_2)$ with λ_1:

$$\left.\frac{d(\Delta x)}{dt}\right|_{x_1} = \lambda_1 \Delta x \tag{13}$$

Thus the perturbation may be expressed as an explicit time domain equation:

$$\Delta x(t)|_{x_1} = \exp\left(\lambda_1 t\right) \tag{14}$$

which has a recovery rate of $\lambda_1 = k(x_1 - x_2)$. On the other hand, a perturbation at the unstable fixed point x_2 would become exponentially increasing.

$$\left.\frac{d(\Delta x)}{dt}\right|_{x_2} = \exp\left(\lambda_2 t\right) \tag{15}$$

where $\lambda_2 = -\lambda_1 = -k(x_1 - x_2)$

It may be seen from the above two equations representing the perturbations at the two

fixed points that their recovery (or blow-up) rates depend on the difference in the values of the parameters x_1 and x_2. At the special case of $x_1 = x_2$, the fixed points exchange stability and the recovery rates tend to zero (Refer to the critical point μ in figures 1 and 2) for an example of the phenomena in two variations of the Pitchfork Bifurcation).

The second question is also answered in the same reference [12]. It explains the increase of autocorrelation and variance when a dynamical system trends towards instability with the help of the example below:

Consider a discrete-time stochastic dynamical system with the vector of state variables being depicted by x. Let x_n depict the value of the state variable vector x at discrete time instance n. Now, if an additive noise say, Gaussian noise, is added to the stochastic dynamical system at every discrete time interval Δt, the slightly perturbed set of state variables, say x_{n+1}, of the otherwise stable dynamical system, would attempt to return to the set of state variables before the perturbation x_n, with an exponential recovery speed.

$$x_{n+1} - x_n = \exp(\lambda \Delta t)(x_{n+1} - x_n) + \zeta_n \sigma \tag{16}$$

where σ is the standard deviation representing the stochastic noise (assumed Gaussian) inherent to the stochastic dynamical system and ζ_n represents a coefficient to σ to model the magnitude of the stochastic noise at discrete-time instant n. λ represents the rate of exponential recovery.

The term $x_{n+1} - x_n$ may then simply be replaced with term y_{n+1} which depicts the deviation of the vector of state variables x between discrete-time instances n and $n+1$.

$$y_{n+1} = \exp(\lambda \Delta t) y_n + \zeta_n \sigma \tag{17}$$

Now if the time intervals between perturbations Δt and the recovery rate λ are independent of the state variables x_n (and therefore their perturbations y_n), the above equation may be rewritten in the form of an autoregression model of the first order:

$$y_{n+1} = \alpha y_n + \zeta_n \sigma \tag{18}$$

The autocorrelation constant $\alpha \equiv \exp(\lambda \Delta t)$ is zero for a purely white gaussian noise and can be one or even greater for other kinds of highly correlated noises in stochastic processes such as brown noise (un-normalized data only).

For the general equation of a lag-1 autoregression:

$$y_{n+1} = \alpha_0 + \alpha y_n + \zeta_n \sigma \tag{19}$$

the expected value (mean) of y_n may be computed using:

$$\mathbb{E}(y_{n+1}) = \mathbb{E}(\alpha_0) + \mathbb{E}(\alpha y_n) + \mathbb{E}(\zeta_n \sigma) \tag{20}$$

or,

$$\mu = \alpha_0 + \alpha\mu + 0 \tag{21}$$

or

$$\mu = \frac{\alpha_0}{1 - \alpha} \tag{22}$$

Thus, if $\alpha_0 = 0$, as in Equation 18, the mean of autoregression μ will also be zero.

The variance of y_n, $\sigma_{y_n}^2$ may be computed using the formula for variance:

$$\sigma_{y_n}^2 = \mathbb{E}(y_n^2) - (\mathbb{E}(y_n))^2 \tag{23}$$

or,

$$\sigma_{y_n}^2 = \mathbb{E}(y_n^2) - \mu^2 \tag{24}$$

For computing the first term of the RHS of Equation 24, Equation 19 may once again be utilized by taking the squares on both of its sides:

$$y_{n+1}^2 = \alpha_0^2 + \alpha^2 y_n^2 + \zeta_n^2 \sigma^2 + 2\alpha_0 \alpha y_n + 2\alpha_0 \zeta_n \sigma + 2\alpha y_n \zeta_n \sigma \tag{25}$$

or,

$$\mathbb{E}(y_n^2) = \alpha_0^2 + \alpha^2 \mathbb{E}(y_n^2) + \zeta_n^2 \sigma^2 + 2\alpha_0 \alpha \mathbb{E}(y_n) + 0 + 0 \tag{26}$$

or,

$$\mathbb{E}(y_n^2) = \frac{\alpha_0^2 + 2\alpha_0\alpha\mu + \zeta_n^2\sigma^2}{1 - \alpha^2} \tag{27}$$

Substituting the value of μ as per Equation 22:

$$\mathbb{E}(y_n^2) = \frac{\alpha_0^2 + 2\alpha_0\alpha\frac{\alpha_0}{1-\alpha} + \zeta_n^2\sigma^2}{1 - \alpha^2} \tag{28}$$

The LHS of Equation 28 and 22 may now be substituted in Equation 24 in order to get:

$$\sigma_{y_n}^2 = \frac{\alpha_0^2 + 2\alpha_0\alpha\frac{\alpha_0}{1-\alpha} + \zeta_n^2\sigma^2}{1 - \alpha^2} - \left(\frac{\alpha_0}{1-\alpha}\right)^2 \tag{29}$$

Putting $\alpha_0 = 0$ as per Equation 18, the final expression for $\sigma_{y_n}^2$ comes out to be:

$$\sigma_{y_n}^2 = \frac{\zeta_n^2\sigma^2}{1 - \alpha^2} \tag{30}$$

As a process (represented by a vector of state variables, such as x) approaches towards a critical bifurcation point, it undergoes Critical Slowing Down in which its recovery rate λ progressively slows down to zero. The slowing down of the recovery of the process from any perturbation causes the perturbations to become progressively correlated (i.e. α increases towards one) and allows unrestricted increase in variance of its perturbations $\sigma_{y_n}^2$ (towards infinity).

Thus the mathematical relationship between Critical Slowing Down and a corresponding increase in both Autocorrelation and Variance was established.

Chapter 4

Offline Analysis

Power grid studies on distribution of frequency deviation/fluctuation aid in developing suitable control mechanisms for power grid operators. Conventionally, the Gaussian model has been used to model its distribution [25], but certain features of real power grids such as heavier tails (i.e. when the PDF of frequency fluctuations at a distance of several standard deviation have a significantly higher magnitude than the corresponding PDF magnitudes of the assumed Gaussian distribution. This is also called as having a high kurtosis), skewness (frequency fluctuations being asymmetric around the mean) and even having bimodal or multimodal distributions are not explained by the simple model. The first part of the 'Offline Analysis' chapter explores this aspect by plotting PDFs of several world power grid frequency archives and visually analyzing the results.

Various frequency time-series archives for a diverse set of real-world grids were obtained and analyzed by plotting their bulk distribution probability density functions and autocorrelation decay functions. The data for most European and US grids was conveniently curated by the authors of [13, 14]. For the other regions of the world, [15, 16] had the data for the Tokyo grid, [17, 18] for the Nordic grids, [19, 20] for Continental European grid and [21] for the UK Grid. All time series were collected at sampling rates between 0.5 seconds (Tokyo) and 10 seconds (Continental Europe). Refer to Table 1 for further details on sampling times and total duration of sampling.

For all grids, the frequency data was:

- plotted as a Probability Distribution Function (PDF)

- used to estimate values for mean μ and standard deviation σ in order to plot the closest fitting Gaussian curve denoted by

$$PDF(f) = \frac{1}{\sigma\sqrt{2\pi}} \exp\left\{-\frac{1}{2}\left(\frac{f-\mu}{\sigma^2}\right)\right\} \tag{31}$$

with the objective of visually checking the level of agreement/disagreement between the

Table 1: Grid-wise sampling data

Grid	Nominal Frequency	Sampling time	Total Sampled Duration	Presented in Fixed Time Autocorrelation Plot?
Continental European (CE)	50Hz	1s	1 year (2019)	Yes
Nordic	50Hz	0.5s	2 years (2018 and 2019)	Yes
Great Britain (GB)	50Hz	0.5s	2 years (2019 and 2020)	Yes
Mallorcan (Spain)	50Hz	1s	3 months (Oct to Dec 2019)	Yes
Western Interconnection (US-WI)	60Hz	1s	7 days (in May 2019)	Yes
Texas (US-TX)	60Hz	1s	3 days (in May 2019)	No
Tokyo	50Hz	1s	5 months (Jan, July, Aug, Oct, Dec 2020)	No
France (RTE)	50Hz	10s	1 year (2019)	No
Indian (NRLDC)	50Hz	30s	6 days (4 days in 2019 and 2 days in 2020)	No

generally used Gaussian curve used to model grid frequency PDFs.

The plotted bulk distribution PDFs visually revealed insights including any deadbands [5, 6] mandated in their grid operation, their skewness, thickness of their tails, etc. A quantitative study of their moments like kurtosis and skewness was not conducted as was done in [2].

In the plotted autocorrelation decay curves, all grids showed exponentially decreasing autocorrelations $c(\tau)$ for smaller values of τ.

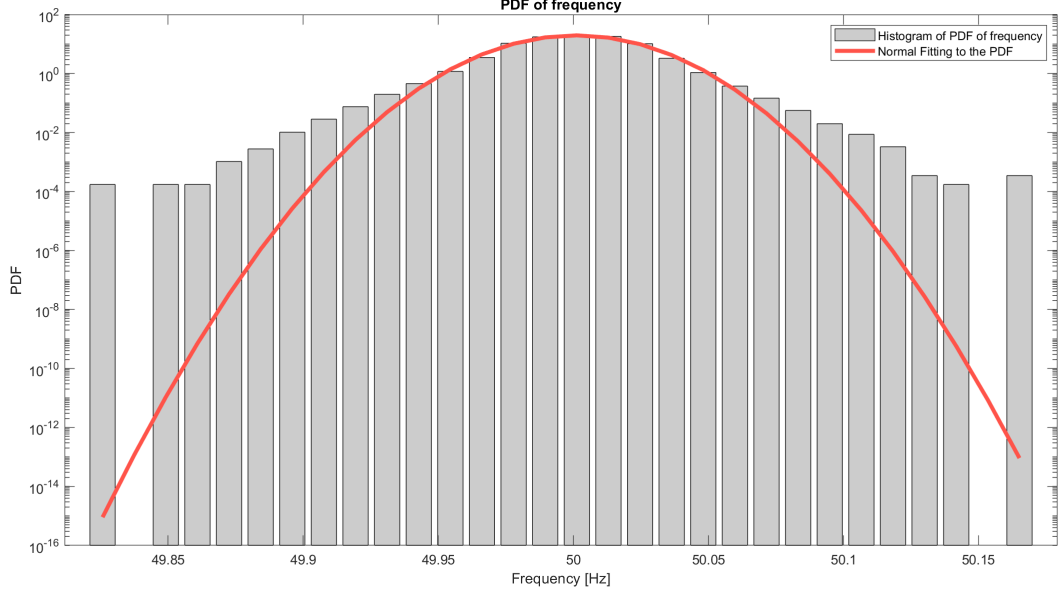$$c(\tau) \propto exp\left(-\frac{\tau}{t_{corr}}\right) \qquad (32)$$

Figure 3: Frequency Probability Density Function plots for the Continental European grid for the year 2019. There is significant deviation of the actual PDF values (grey bars) from the closest Gaussian model fitted to the same data (red curve) at the tails, which are much heavier in the former.

where t_{corr} is the correlation constant for the grid (the time period in which autocorrelation decays to $\frac{1}{e}$th of its original value). This is in agreement with the usual autocorrelation decay trends observed for natural stochastic processes, such as the Ornstein-Uhlenbeck Process [26]. Instead of the autocorrelation decay constant t_{corr}, sometimes its reciprocal, inverse-time autocorrelation decay constant $\frac{1}{t_{corr}}$ or simply t_{corr}^{-1} is used. In order to confirm if the decrease was indeed exponential with a grid-specific inverse-time autocorrelation decay constant, semi-log graphs ($\log(c(\tau))$ vs τ) were also plotted. The decay constants were computed by calculating the slopes of the semi-log graphs and it was found that the grids which were bigger, more robust and showed bulk distribution PDFs which were less-deviating from Gaussian distributions, had greater values of inverse-time correlation t_{corr}^{-1}. This parameter can also be construed as α, the relative damping strength of the grid for small oscillations and can be an indicator of the overall robustness of the grid. Refer to Table 2 for the computed values.
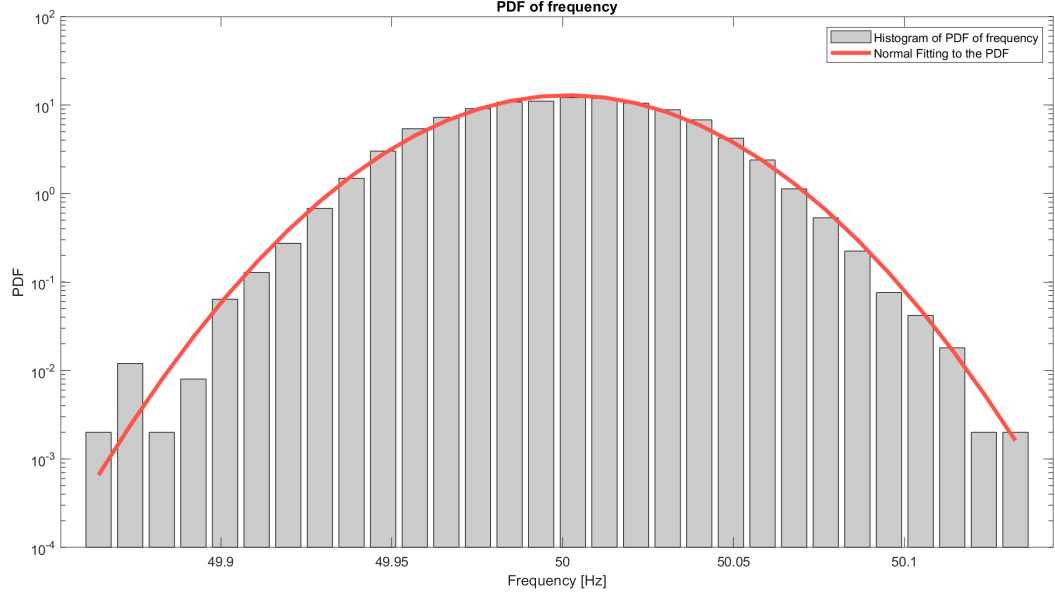
(a) Frequency Probability Density Function plots for the Tokyo grid for January 2020.
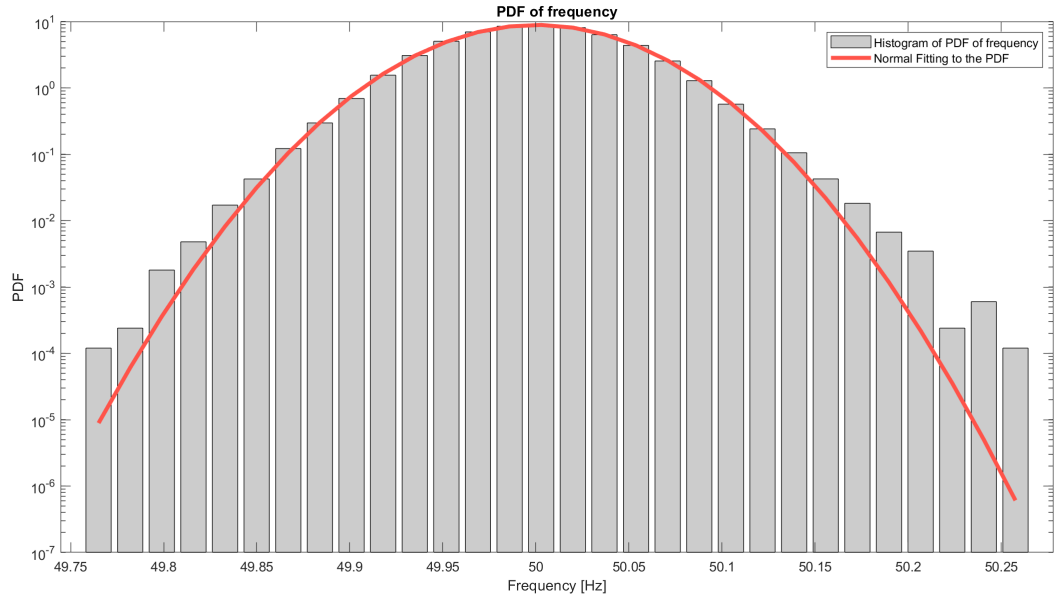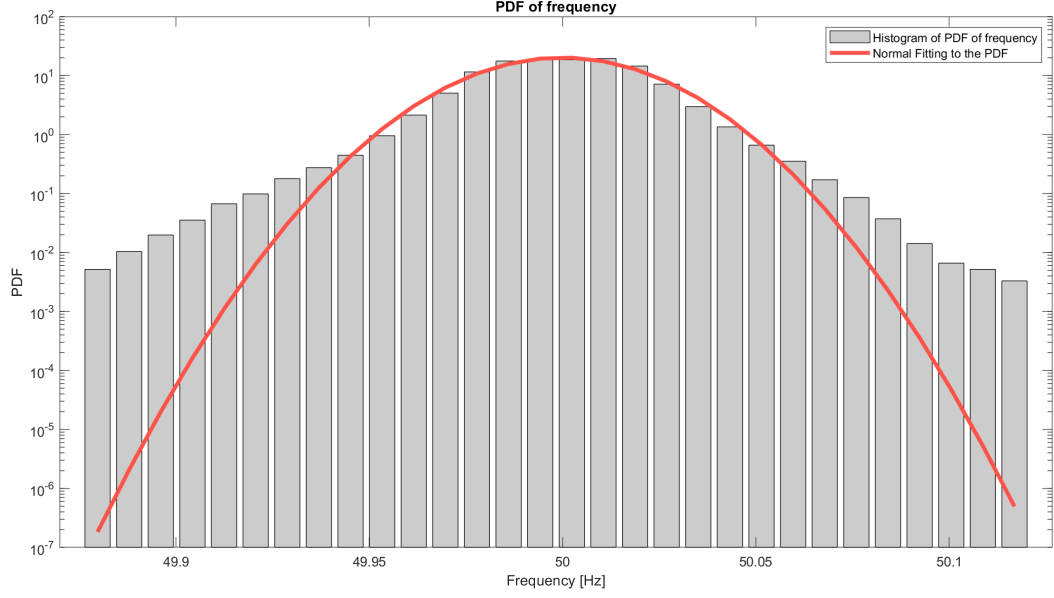

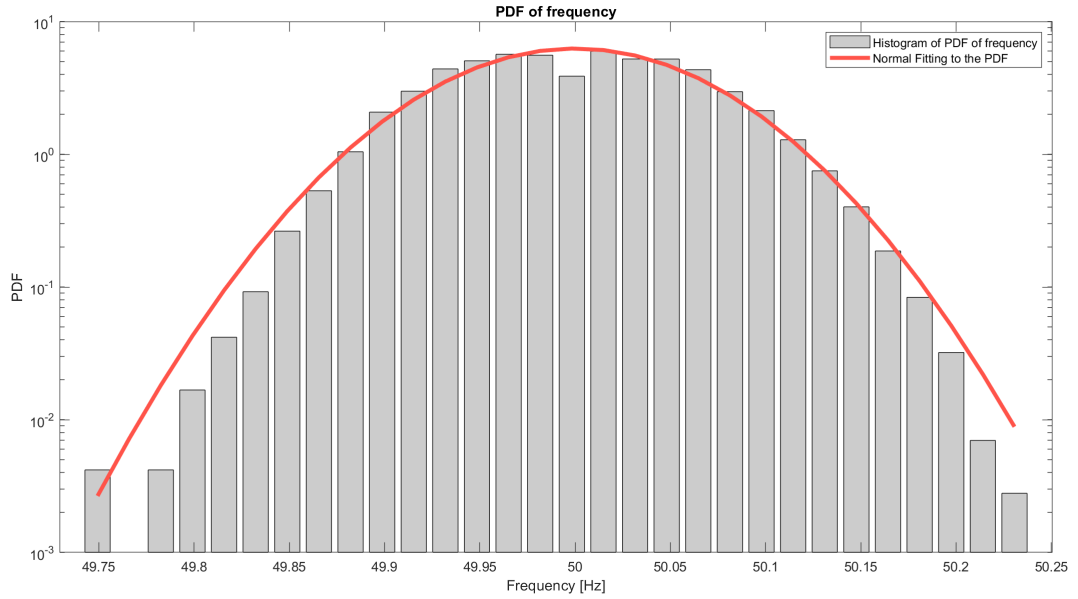(b) Frequency Probability Density Function plots for the Nordic grid for the year 2019.

Figure 4: Frequency distribution PDFs of some grids show almost identical characteristics to the Gaussian Distribution. For the case of Tokyo and Nordic grids, there is a fair level of agreement between the actual PDF values (grey bars) and the closest fitted Gaussian model (red curve). An assumption of Guassianity, for some grids, therefore is not completely unfounded.

Effect of sampling duration on consistency of offline analysis of data

Different grids can have their own set of 'events', such as firing up of boilers or other kinds of switching events, or 'cycles' of changes, such as sub-hourly power dispatches, semi-diurnal
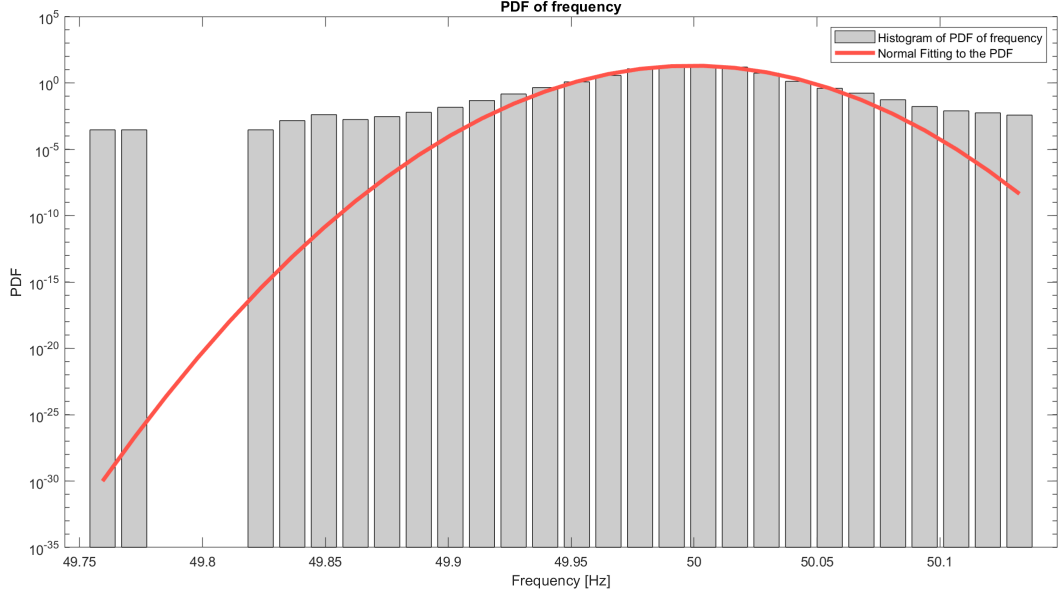
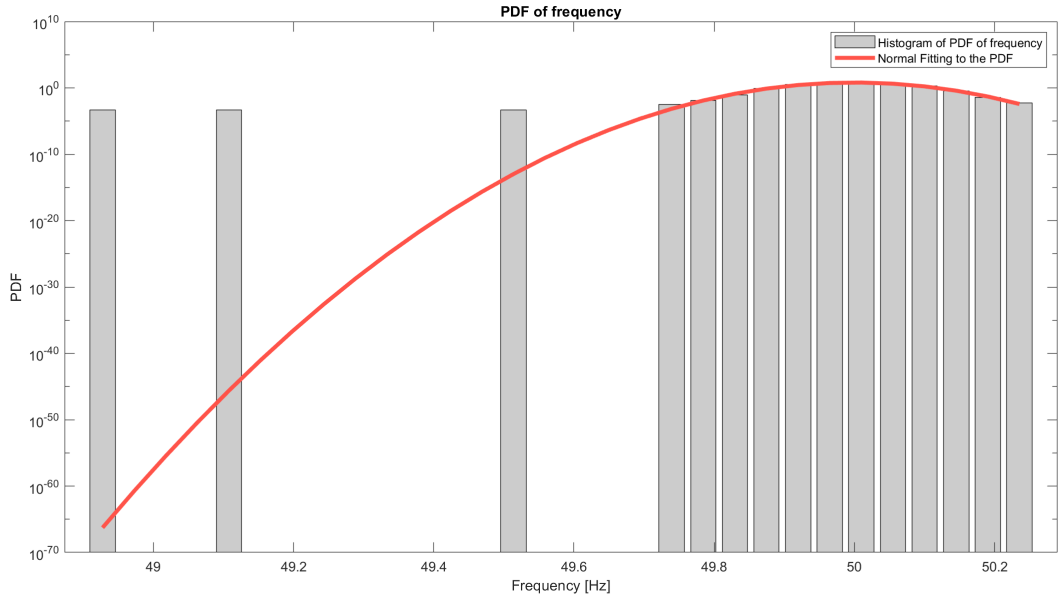(a) Frequency Probability Density Function plot for the French RTE grid for September 2019.

(b) Frequency Probability Density Function plot for the Great Britain grid for April 2020.

Figure 5: Some sets of grids show an appreciable level of deviation from the Gaussian distribution in that: they have heavier tails, such as for the French RTE Grid, or they have a bimodal distribution (two peaks), such as for the Great Britain Grid.

variation in solar generation, hourly wind power fluctuations, etc. A question then arises: Can the 'statistical nature' of a grid be really generalized if it itself doesn't show a constant characteristic in its dynamics? The answer is: Yes, but only if a 'sufficient' duration of data has been collected for analysis, such that all kinds of cyclical variations are 'averaged-out'

(a) Frequency Probability Density Function plot for the French RTE grid for January 2021.

(b) Frequency Probability Density Function plot for the Great Britain grid for August 2019.

Figure 6: Blackouts are easily singled out in visual post mortem analysis of grid frequency PDFs. A frequency PDF of a grid plotted for a time duration incorporating a blackout is generally too anomalous from the 'usual' non-blackout PDFs. In the above plots, the severe outliers in the PDFs of the French RTE and the Great Britain grids were the results of occurrence of a 10 minute blackout on 08 January 2021 and a 5 minute blackout on 09 August 2019 respectively.

over the duration, displaying a somewhat consistent statistical signature irrespective of the actual time the analysis was made or data collected from.
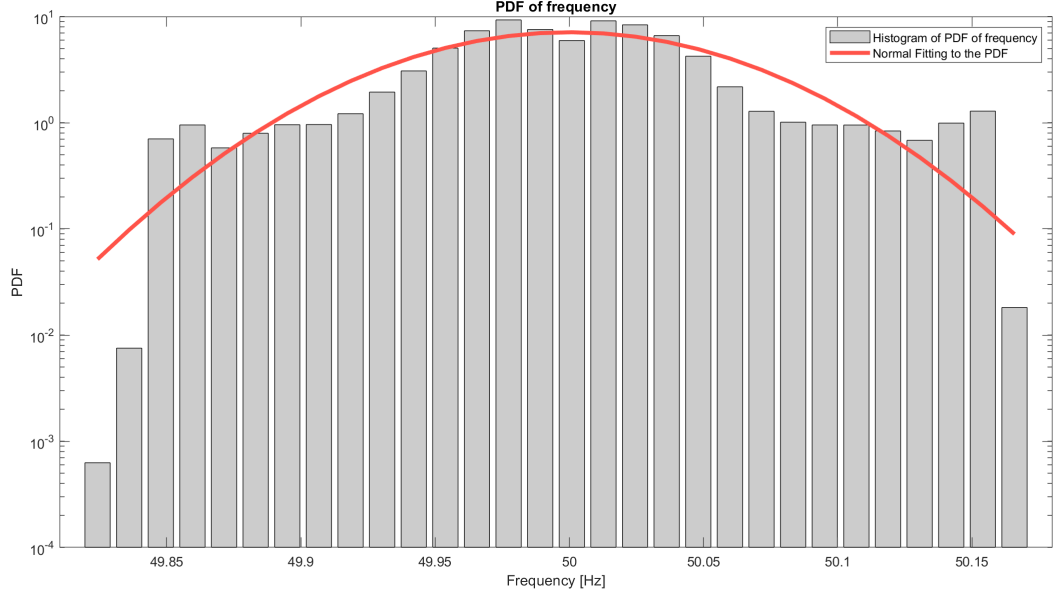
Figure 7: Frequency Probability Density Function plots for the Spanish Mallorcan grid for the May 2019. There is high degree of deviation of the actual PDF values (grey bars) from the closest Gaussian model fitted to the same data (red curve). Apart from the heavier tails, the frequency distribution appears to have multiple peaks.

Data for different years or months of select grids (Great Britain, France RTE, Nordic, Japan) mentioned in Table 1 were compared in terms of their Fixed Time Autocorrelation plots (Autocorrelation Decay Curves). The plots were a mixture of year-wise (Nordic), month-wise (Great Britain, France RTE, Tokyo) and day-wise (Indian NRLDC) data. It was concluded that, barring some small vertical shifts among the autocorrelation values, the trends were consistently displayed for year-wise and month-wise plots, but did not show consistency in their day-to-day plots.

Data for six non-continuous days (07 April 2019, 03 July 2019, 08 August 2019, 14 December 2019, 01 February 2020 and 05 April 2020) for the Indian grid (NRLDC) was also compared in a similar fashion. Some of the days have also been marked with attributes to indicate notable demand-generation characteristics associated with the day, including: Day with minimum renewable generation, Day with maximum renewable generation contribution (07 April 2019), Day with minimum solar power contribution (08 August 2019), Day with lowest power demand (14 December 2019) and Day with lowest renewable generation contribution (01 February 2020). The plots were inconsistent and therefore a day's worth of data could be considered insufficient to average-out all the dynamic differences in a grid's
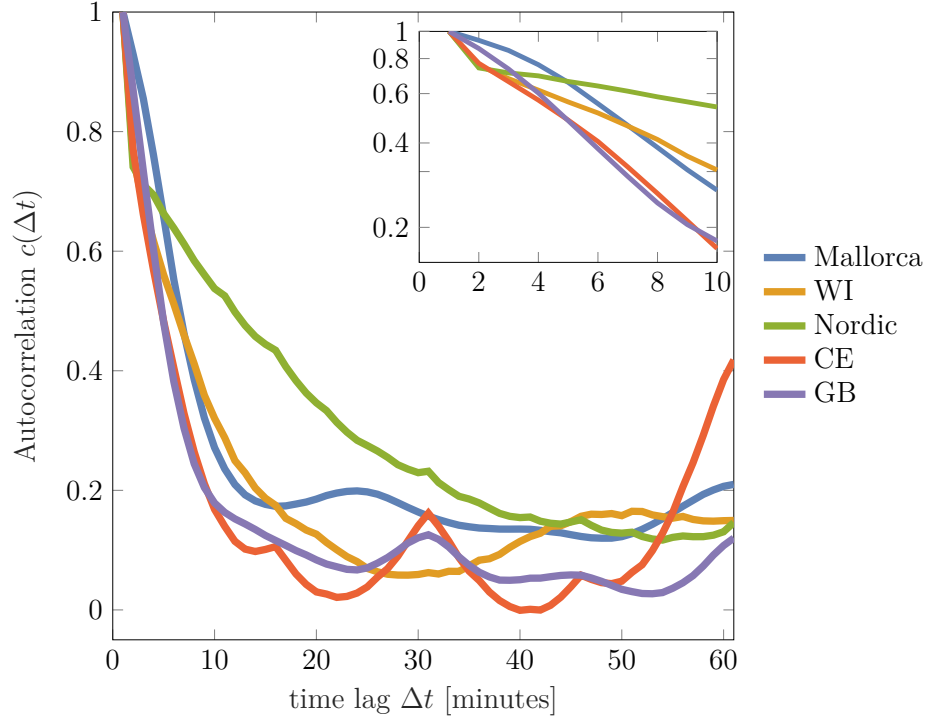
Figure 8: Fixed Time Autocorrelation plots for five different power grids. The different rates of exponential decay in autocorrelation values indicates the difference in their relative damping strengths. The Continental European and Great Britain grids display peaks every 15 minutes which may be explained from their energy dispatch routine.
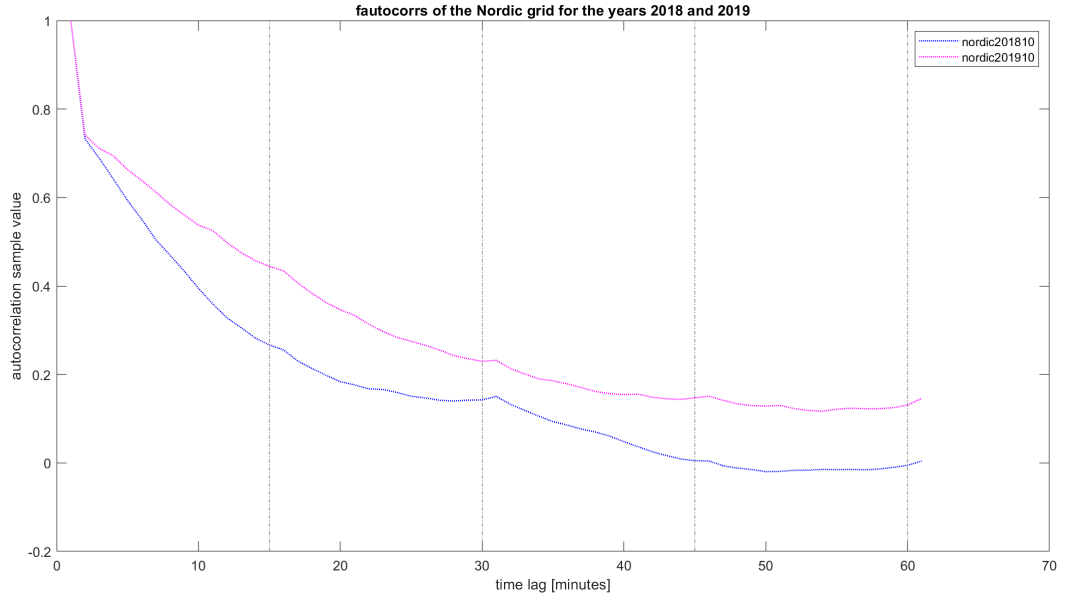

Figure 9: Fixed Time Autocorrelation plots for the Nordic Grid for two consecutive years, 2018 and 2019. They present a fairly consistent picture of the grid's dynamics, with only a minor difference in the magnitude of the autocorrelation values.

20

Table 2: Inverse-correlation time t_{corr}^{-1} values for different grids. These values were obtained by plotting the Fixed Time Autocorrelations of various grids in Figure 8 in a semi-log graph and obtaining the decaying slopes for the first ten minutes of lag τ. These values can also be likened to the damping ratios of the grids, i.e. how robust/susceptible a grid is to instabilities.

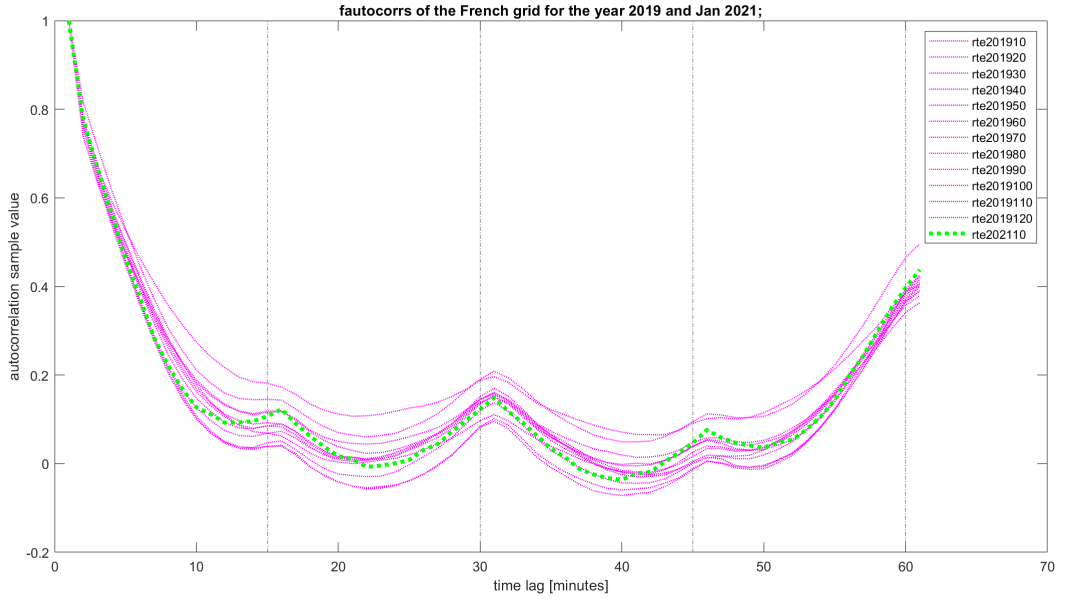| Grid name	Inverse-correlation value t_{corr}^{-1} $[min^{-1}]$
Mallorca	0.0654
Western Interconnection	0.0498
Nordic	0.0235
Continental Europe	0.0829
Great Britain	0.0879

Figure 10: Fixed Time Autocorrelation plots for the French Grid for twelve months of the year 2019 and January 2021. They present a fairly consistent picture of the grid's dynamics.

statistical signature.

Similarly, for smaller total sampling durations, the bulk distribution frequency PDF plots are also susceptible to outliers and therefore not ideal for modelling the grid frequency distributions. For example, the available data for the Western Connection Grids and the Texas Grid, both from USA, was small at 3 days and 7 days respectively.

Thus a minimum of one month could be considered a sufficient duration to model the bulk characteristics of a grid.
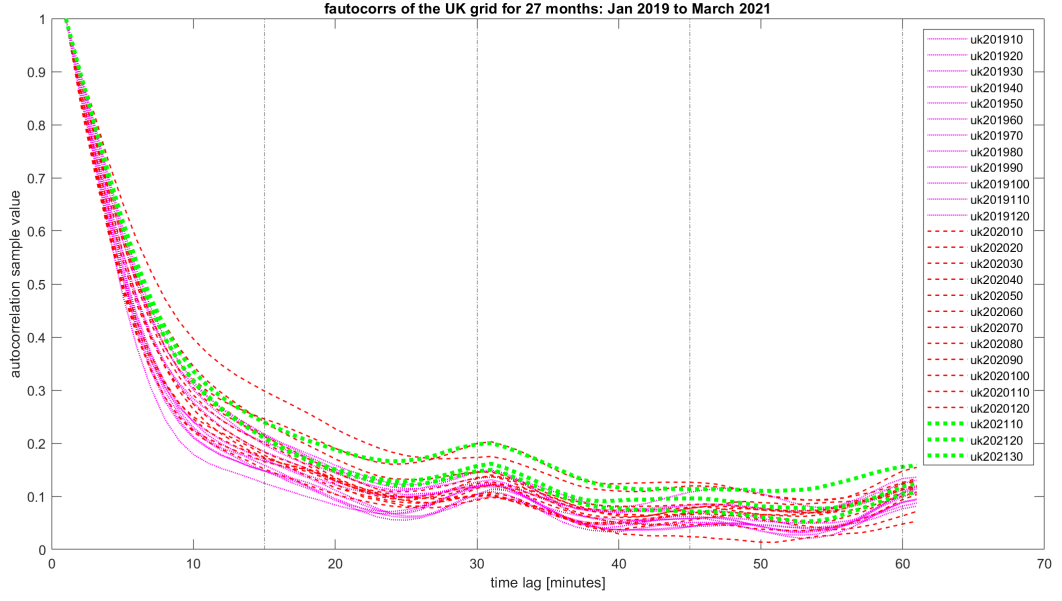
Figure 11: Fixed Time Autocorrelation plots for the Great Britain Grid for twenty seven continuous months, from January 2019 to March 2021. They present a fairly consistent picture of the grid's dynamics.
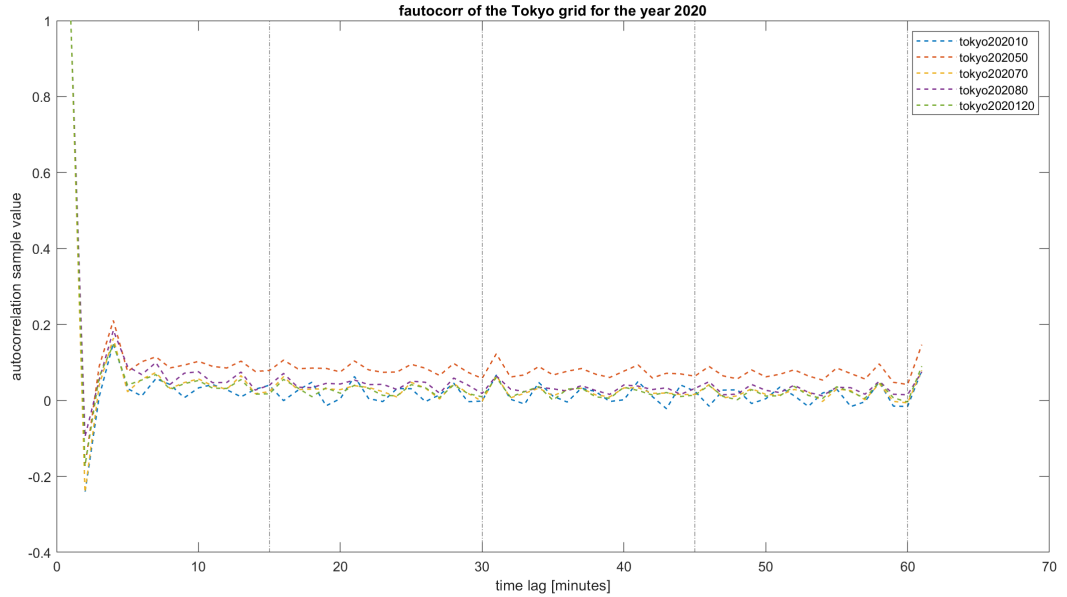

Figure 12: Fixed Time Autocorrelation plots for the Tokyo Grid for five non-continuous months of the year 2020: January, May, July, August and December. They present a fairly consistent picture of the grid's dynamics.
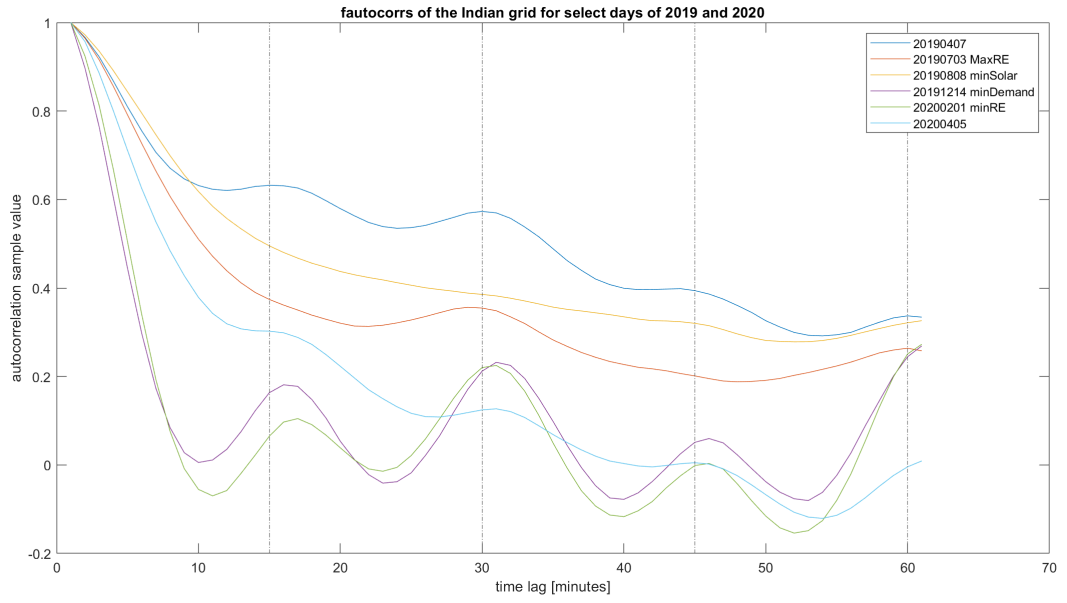
22

Figure 13: Fixed Time Autocorrelation Plots for Six non-continuous days of the Indian Grid: 07 April 2019, 03 July 2019, 08 August 2019, 14 December 2019, 01 February 2020 and 05 April 2020. Some of the days have also been marked with attributes with notable demand-generation characteristics associated with the day.
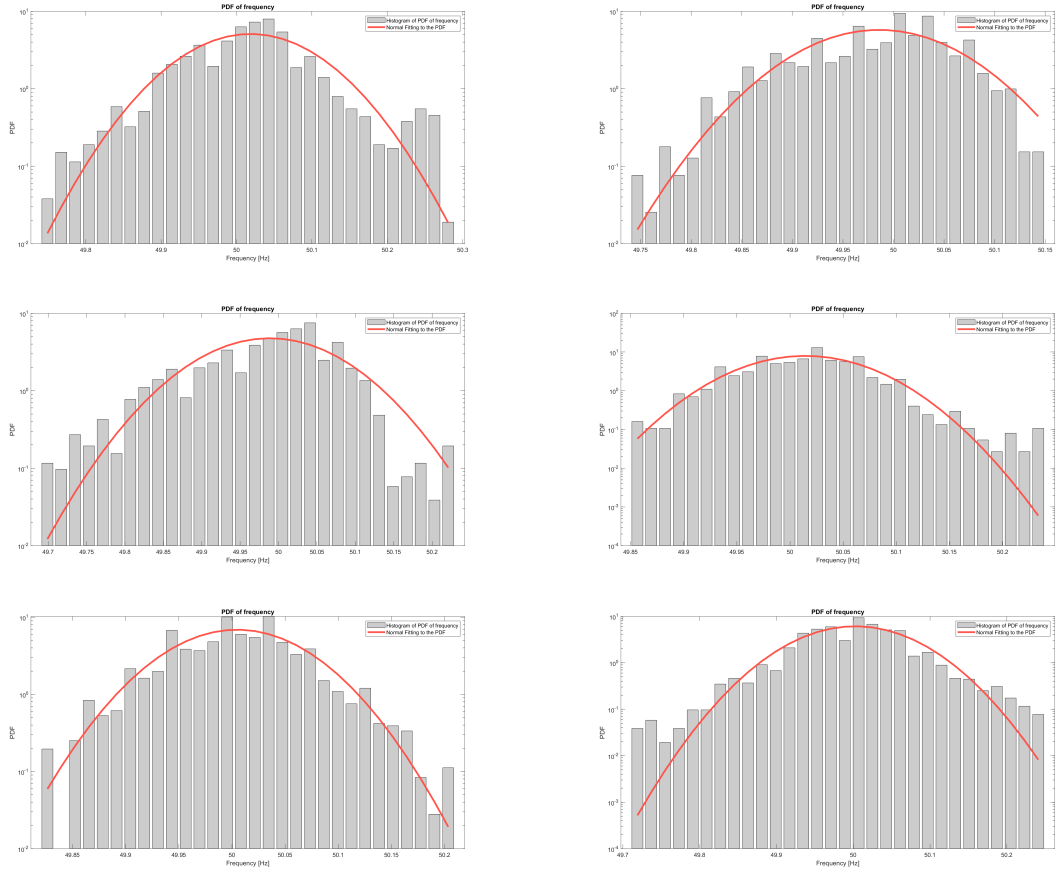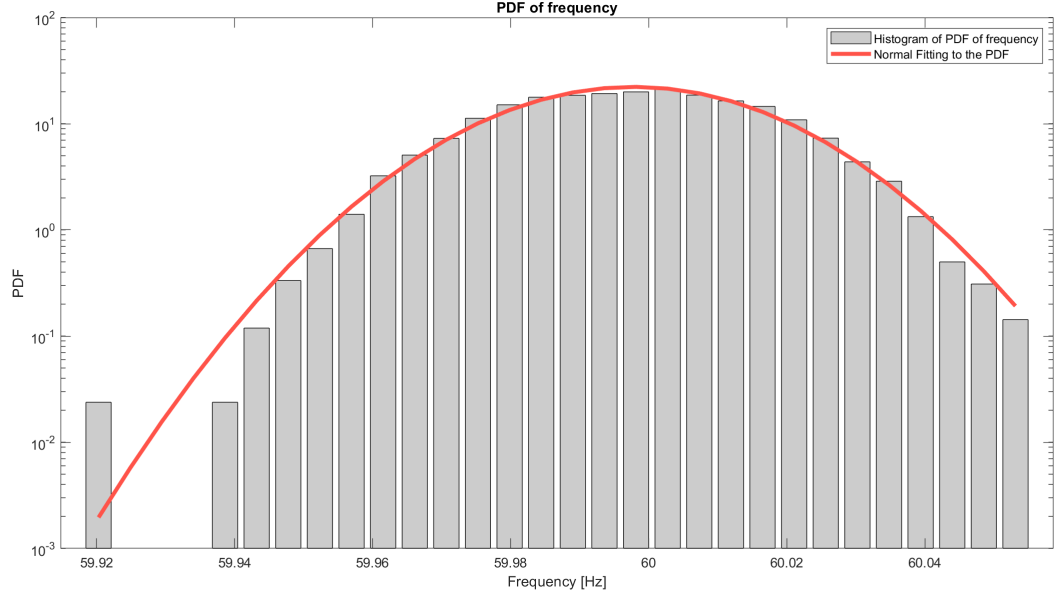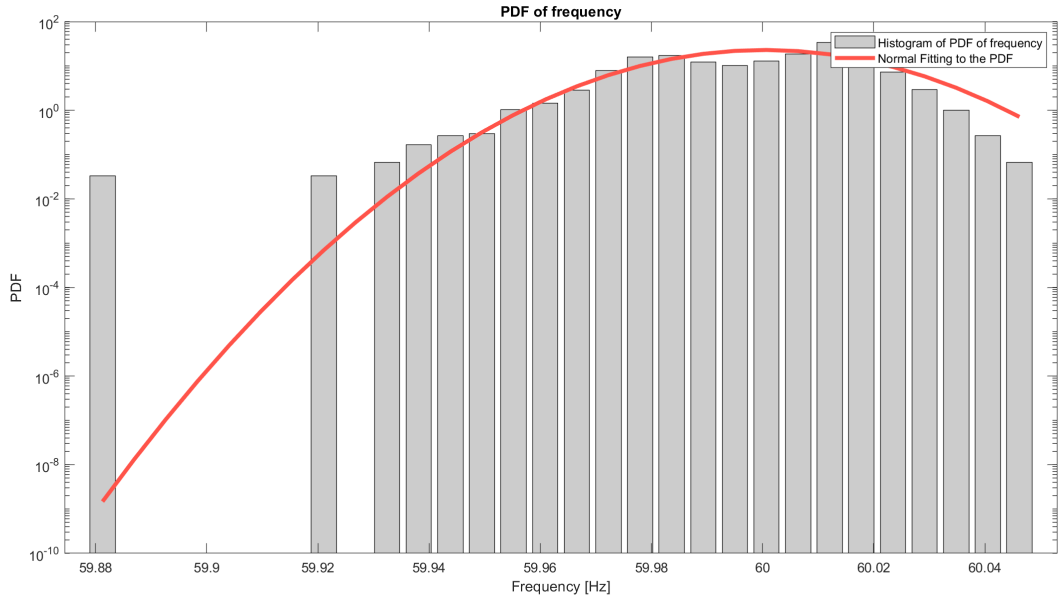
Figure 14: Frequency Probability Density Function Plots for six non-continuous days of the Indian grid (NRLDC). The frequency PDFs show considerable difference among themselves.

(a) Frequency Probability Density Function plot for the Western Interconnection grid in USA for 7 days of May 2019.

(b) Frequency Probability Density Function plot for the Texas Grid for 3 days of May 2019.

Figure 15: The Texas and Western Interconnection grid frequencies both show outliers in the distribution PDFs, despite not having any faults or major incidences during the sampling period. If the total sampled durations are too low, the frequency distribution PDFs are too susceptible to any major fluctuations, and therefore not reliable models to assume the actual grid frequency distribution PDFs on.

Chapter 5

Online Analysis

On similar lines as [7, 8], test were conducted for checking if the symptoms of Critical Slowing Down could be detected by a real-time/online analysis of the state variables of a power grid. In other words, can computing the autocorrelation and variance of real-time PMU data processed over a running window function appropriately as Early Warning Signs of an impending approach instability.

Bifurcation Theory states that a small change in system parameters, such the governor reference power for a generator (P_{Gen}) at certain points, can lead to major upsets in the stability of the power grid. We ran a simulation in which a system was purposefully stressed (via a near constant linear load increment) as time progressed but many restrictions/safety mechanisms were lifted with the aim of singling-out the cause of bifurcation to a change in P_{Gen}(s), in order to best demonstrate that the proposed statistical mechanisms (computing autocorrelations and variances) function well as Early Warning Signs even for slow and steady variations of loads, and not just for sudden changes in state variables caused due to reactionary corrective protection mechanisms or the machines not being given 'free-range' for chasing load increments due to specified safety limits on maximum allowed generated powers. Below is the set of special conditions used for the simulation of the IEEE 9 Bus system:

**Steps and Conditions for Simulating the IEEE 9 Bus System towards instability:**

1. The three load points of the system (Buses 5, 6 and 8) were linearly increased in time, at a rate of $\Delta P\%$ per minute plus a small white noise component $\mathcal{N}(0, \sigma_v)$, with every increment happening at Δt time intervals.

$$P_{L_i}(t + \Delta t) = P_{L_i}(t) * \left(1 + \frac{\Delta P_{L_i}}{100} \right) + \mathcal{N}(0, \sigma_v) \tag{33}$$

Here, ΔP_L values were assigned randomly between $8 - 12\%$ for every load bus, $\sigma_v = 0.01$ and $\Delta t = 0.1$ seconds.

2. Simulation ODE solver solves for the new state variables for the system every 0.01 seconds or $t_{sampling} = 0.01$ seconds. This means that the simulation output can be likened to a stream of PMU data whose sampling rate is 100 Hz or $f_{sampling} = 100$ Hz.

3. Protection mechanisms were disabled. No remedial/corrective action was taken for any drop in bus voltages/grid frequency or any increase in line currents/MVAs.

4. 'Dummy' governors were placed on the three generators (at buses 1, 2 and 3) which could respond instantly to load changes by changing the set reference generation powers P_{Gen}(s) with zero time lag.

5. The generator limits for $P_{Gen_{MAX}}$, $Q_{Gen_{MAX}}$, etc. were removed. Thus the generators had complete freedom to 'chase' the load increments at the load buses, including factoring in the extra line-losses.

Based on the above conditions, simulations were run in PSSE. The simulations ran for about two minutes before the grid 'blacked out' i.e. PSSE solver returned the message 'Network Not Converged' as the continuously increasing loads could not be handled by the generators while maintaining synchronism. The outputs of the state variables, including Demand/Load Powers, Generated Powers, Bus Frequencies, Bus Voltages, Line Currents and Line MVAs have been presented below in Figure 16.
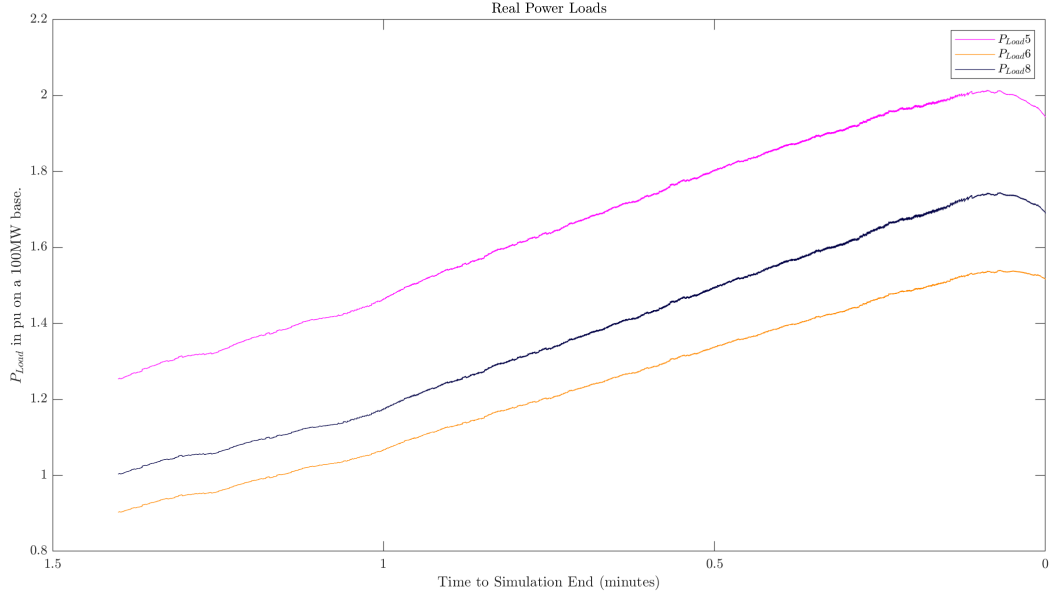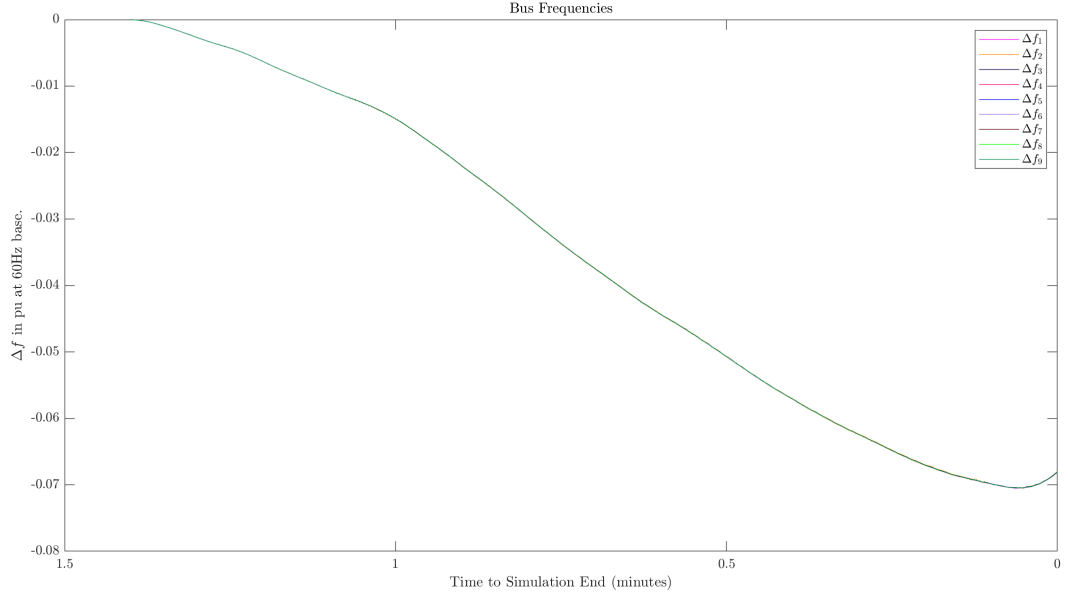
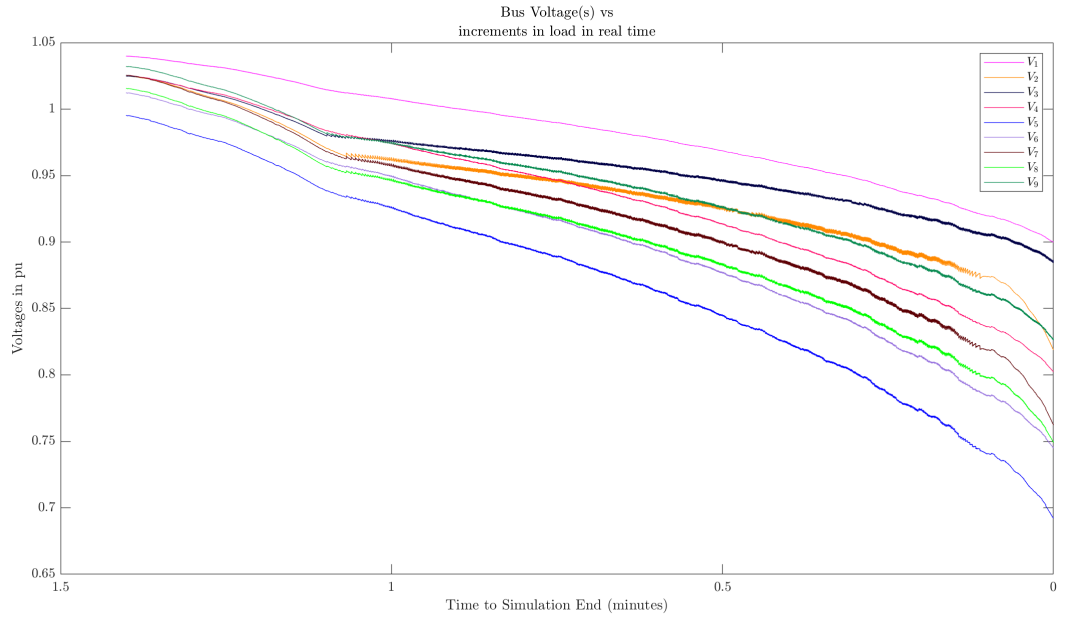(a) Real Power Loads for the simulated IEEE 9 Bus System vs simulation time.
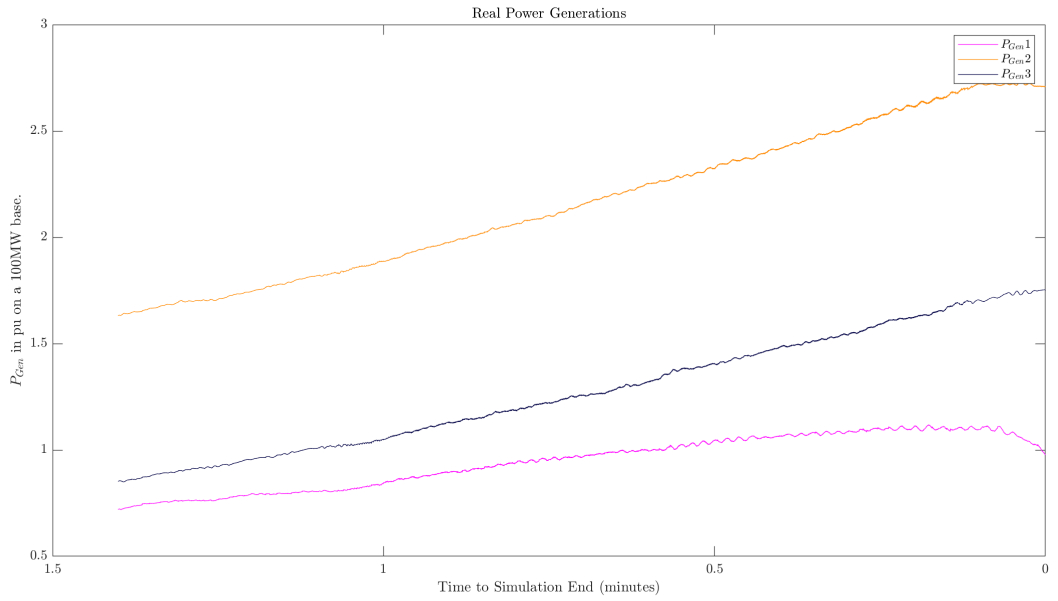
(b) Generated Real Powers for the simulated IEEE 9 Bus System vs simulation time.

Figure 16: Simulation results of the IEEE 9 Bus System as per the prescribed conditions.

(a) Bus Frequencies for the simulated IEEE 9 Bus System vs simulation time.

(b) Bus Voltages for the simulated IEEE 9 Bus System vs simulation time.

Figure 17: Simulation results of the IEEE 9 Bus System as per the prescribed conditions.

(a) Line Currents for the simulated IEEE 9 Bus System vs simulation time.

(b) Line MVAs for the simulated IEEE 9 Bus System vs simulation time.

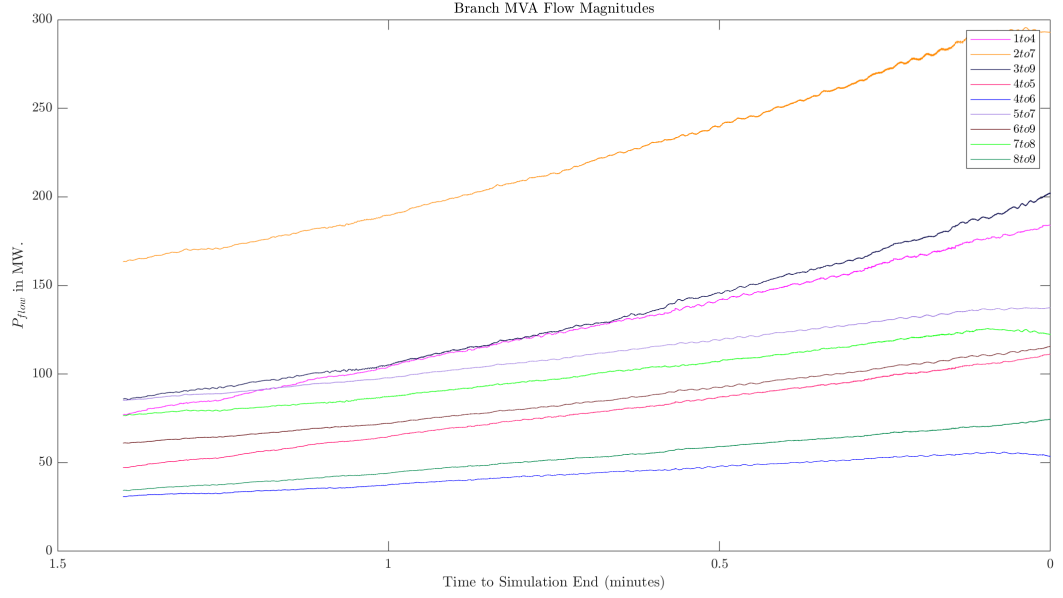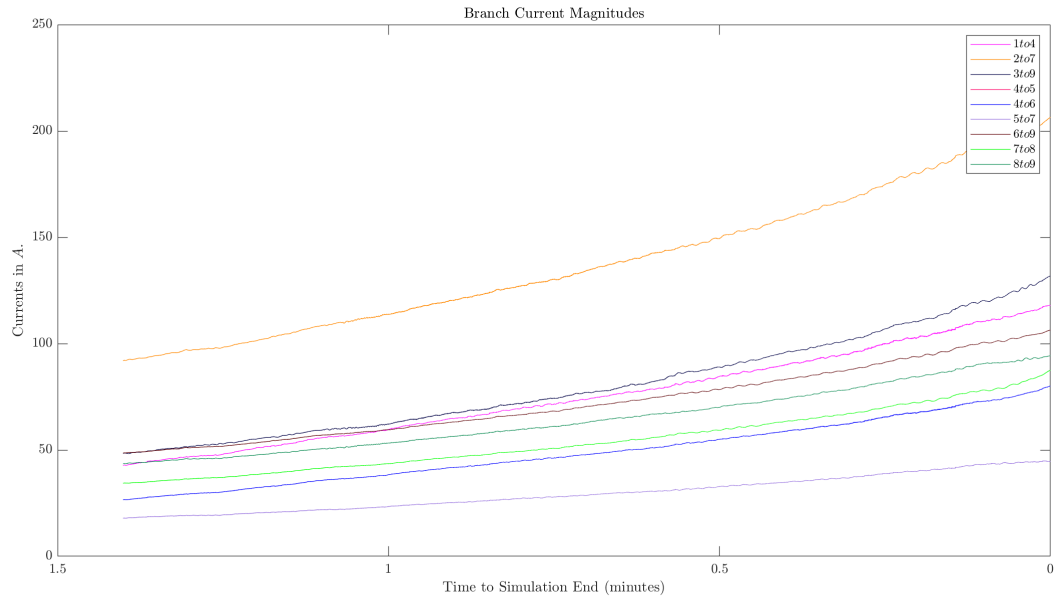Figure 18: Simulation results of the IEEE 9 Bus System as per the prescribed conditions.

Steps for Measuring Critical Slowing Down in the Simulation

1. Choosing a state variable to test for symptoms of Critical Slowing Down on. In this case, Bus Voltages were used to test the same. In the case of the IEEE 9 Bus system, the voltages were $V_1(t), V_2(t) \dots V_9(t)$ in continuous-time or $V_1[n], V_2[n] \dots V_9[n]$ in discrete-time.

2. For real-time evaluation of a time-series in which the entire time-series is obviously unavailable at the current moment (unlike in the Offline Analysis), a running window of length T seconds in real-time or alternatively W instances in number of consecutive discrete-time readings of the chosen state variables (bus voltages) could be used for making analysis. In this thesis, $T = 15$ seconds ($W = 1500$ instances, as $W = \frac{T}{t_{sampling}}$ or $W = \frac{T}{f_{sampling}}$) was chosen.

3. All instances of the bus voltages 'covered' by the current window were:

   (a) Detrended via a Gaussian Kernel Smoothing function.
   Detrending a time-series, i.e. filtering out only the fluctuations in the time-series for analysis and rejecting the long-term slow trends is required for examining Critical Slowing Down as autocorrelation is meant for computation on detrended data, not on raw data, for effective analysis. The detrending was done by first passing the state variables (bus voltages) through a low pass filter, in this case, the Gaussian Kernel Smoothing filter and the resultant 'smoothed' bus voltage signal were then subtracted from the original bus voltage signals.

   $$GKS(n, \sigma_f) = \frac{1}{\sigma_f \sqrt{2\pi}} \exp\left(-\frac{n^2}{2\sigma_f^2}\right) \tag{34}$$

   where σ_f is chosen in order to ascertain the bandwidth of the Low pass filter, such that only slow acting trends of the original bus voltage signals remain in the smoothed signals. In this case, σ_f was taken to be 10. The detrended bus voltage signals were then obtained by subtracting the filtered signals from the original:
   $$d(V_i[n]) = V_i[n] - GKS(V_i[n]) \tag{35}$$

   for the ith bus. The resultant detrended bus voltages may be viewed in Figure 19.

   (b) Subsequently, Fixed Lag Autocorrelation (with Lag $\tau = 1$ second) and Variance were computed over the detrended bus voltages. The autocorrelations were computed using `AR` function and variances were computed using the `var` function in MATLAB 2022a. Refer to Figure 20 for the results.

   (c) Lastly, in order to statistically test for serial dependence of the autocorrelation and variance data (i.e. whether they are significantly increasing wrt time to be actually considered to be symptoms of Critical Slowing Down), a new kind of statistical parameter, namely the Modified Kendall's Tau Correlation Coefficient was computed over both of the previously computed Fixed Lag Autocorrelation and Variance values. In order to explain this new parameter, firstly the regular

Kendall's Tau Correlation Coefficient is briefly introduced:

$$\text{Kendall's } \tau = \frac{\text{Number of Concordant Pairs} - \text{Number of Discordant Pairs}}{\text{Total Number of Pairs}}$$

(36)

where, For a discrete-time series, such as $V_i[n]$ in the case of this thesis, a Concordant pair in a time series refers to two discrete-time instances p and q with $p < q$ such that $V_i[p] < V_i[q]$. Similarly, Discordant pairs refer to the cases where $V_i[p] > V_i[q]$. Note that i only refers to the bus number in the IEEE 9 Bus System.

Kendall's Tau Correlation Coefficient is valued between -1 and 1, but also has an associated p-value, which measures the confidence of the null hypothesis that the serial dependence of a time-series is statistically significant. Sometime, the p-value is not statistically significant (p-value > 0.05) but applying Kendall's Test still outputs a correlation coefficient value, making the test equivocal. Thus to accommodate for the confidence interval along with the obtained correlation coefficients, a new parameter for testing the serial dependence of data, namely the Modified Kendall's Tau Correlation Coefficient (or MKTCC in short) was used to test if the increases in Fixed Lag Autocorrelations and Variances were statistically significant:

$$\text{Modified Kendall's } \tau' = -\tau \log\left(\text{pVal}_\tau\right)$$

(37)

In Figure 21, it can be observed how the MKTCC value of their autocorrelation and variance values shoot up faster than those of others. While in this thesis, this observation was not continued with in a rigorous quantitative analysis, this statistical parameter seems promising as an early warning sign indicator of proximity to instability for a power grid, and identifying areas in the grid which are the most vulnerable to instabilities caused by steadily increasing stochastic variations in load.

4. Next the window is moved by a length equivalent to T_{moving} seconds or W_{moving} discrete time instances. In this case, $T_{moving} = T/10$ or $T_{moving} = 1.5$ seconds (and therefore $W_{moving} = 150$ discrete-time instances).

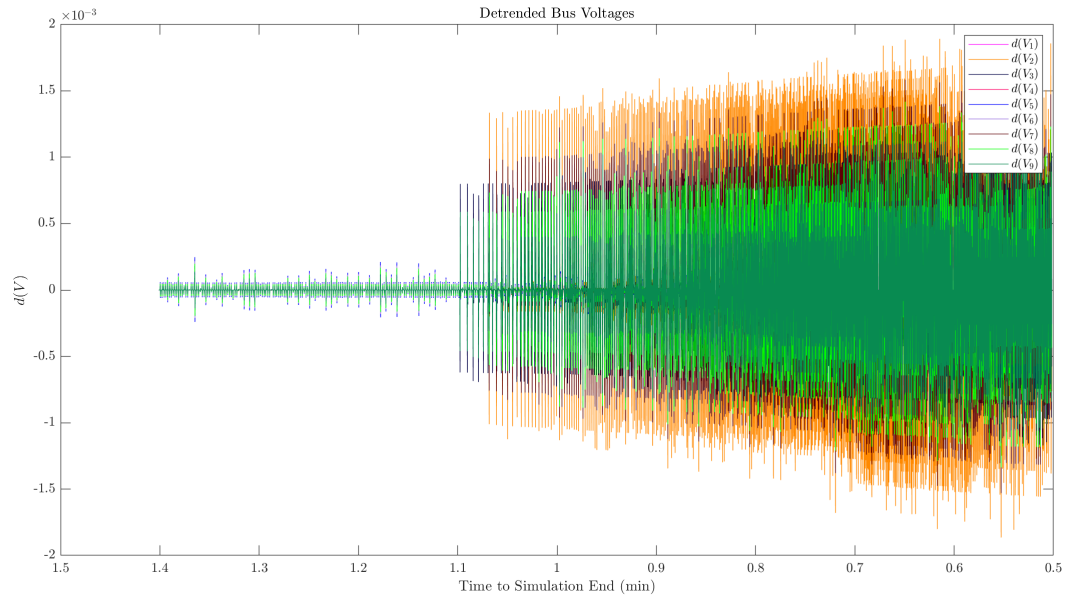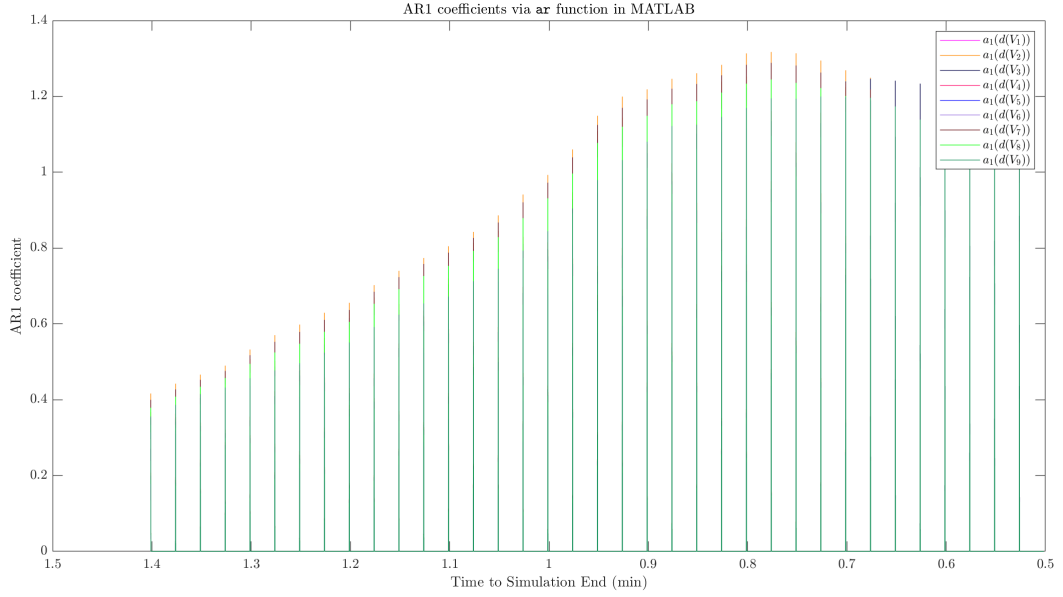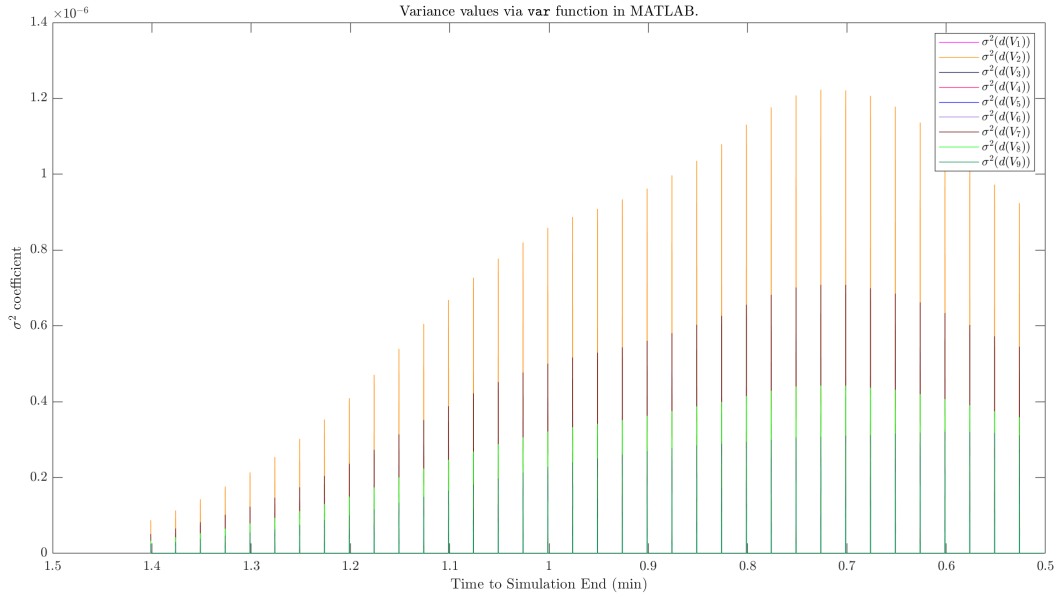5. Goto Step 3 until simulation ends.

Figure 19: Detrended Bus Voltages for the simulated IEEE 9 Bus System vs simulation time.

(a) Fixed Lag Autocorrelations (un-normalized) with Lag $\tau = 1s$ computed for the Detrended Bus Voltages for the simulated IEEE 9 Bus System vs simulation time.

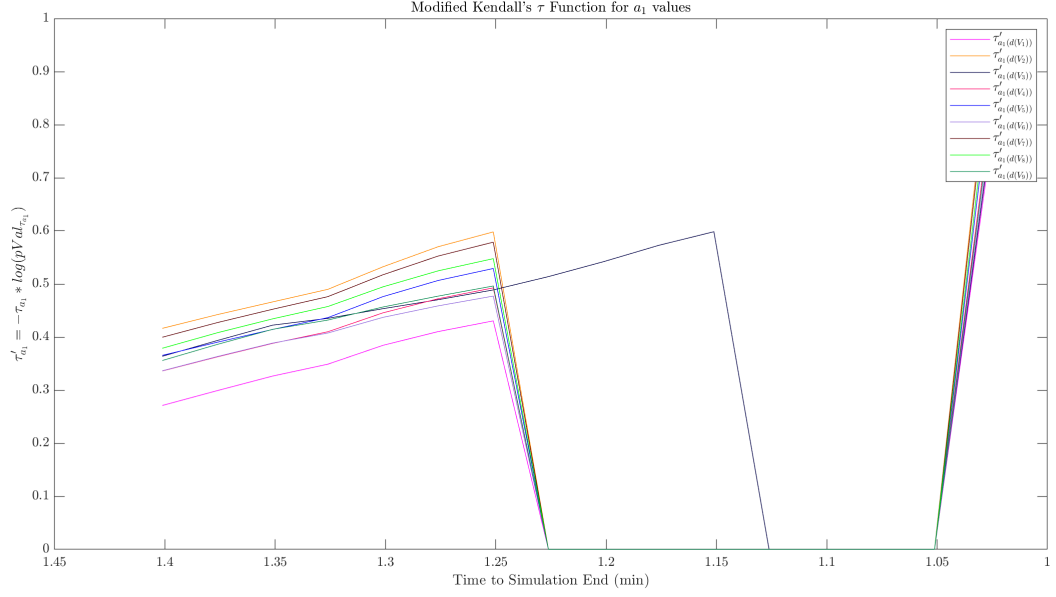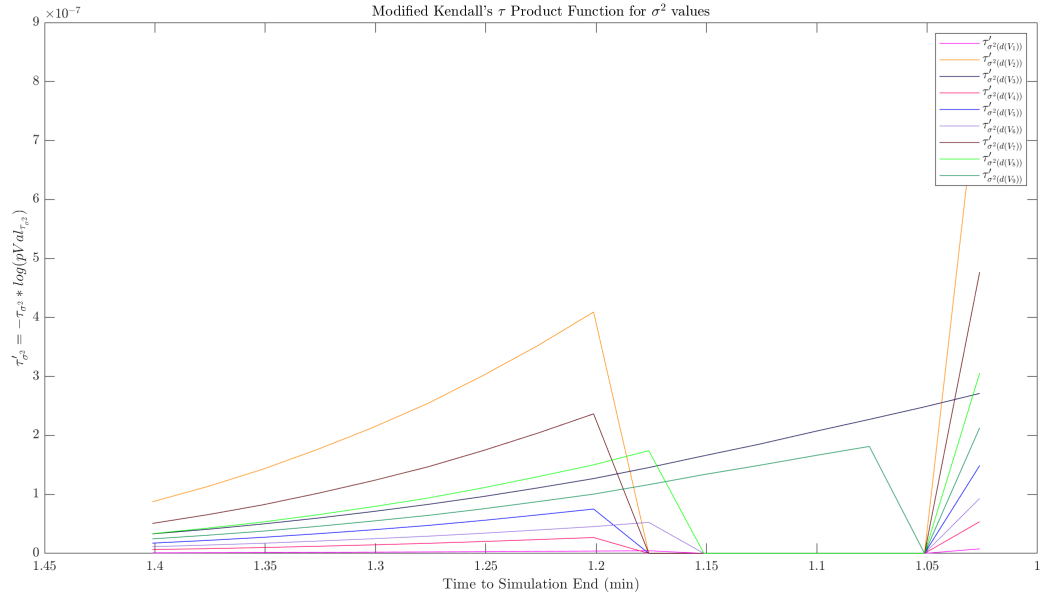(b) Variances computed for the Detrended Bus Voltages for the simulated IEEE 9 Bus System vs simulation time.

Figure 20: Data Analysis done on the Bus Voltages resulting from the IEEE 9 Bus System Simulation for the purpose of testing if the system shows symptoms of Critical Slowing Down.

(a) Modified Kendall's Tau Correlation Coefficients (MKTCC) computed for the previously computed Fixed Lag Autocorrelations of the Detrended Bus Voltages.

(b) Modified Kendall's Tau Correlation Coefficient (MKTCC) computed for the previously computed Variances of the Detrended Bus Voltages.

Figure 21: Modified Kendall's Tau Correlation Coefficient was used for checking for any serial dependence of the autocorrelation and variance data, i.e. if the increases in both parameters was statistically significant or not.

Continuous stress on the power grid in the form of a constantly increasing power demand on the generators is bound to cause a blackout in the grid. In simulation terms, this is when the 'Network Not Converged' error message is thrown by PSSE, and in mathematical terms, this phenomenon is called as Critical Bifurcation. It was verified using visual inspection of the Fixed Lag Autocorrelation plots, Variance plots and their respective Modified Kendall's Tau Correlation Coefficient plots that Fixed Lag Autocorrelation and Variance of Bus Voltages are suitable early warning signs for indicators to instability in the power grids, predicting the critical bifurcation event a minute earlier. It may be noted that the time by which an advanced prediction of an impending critical bifurcation is does not carry much meaning without accommodating the size of the grid and the degree of load demand stress on the grid. Other simulations were done with lower stress (5% to 7% increase in demand power per minute) whose analysis would lead to an earlier prediction of the impending critical bifurcation (around several minutes before the event). Similarly, a higher stress (25% per minute) could only be diagnosed around thirty seconds earlier. Ultimately, the figure of interest is the ratio of the time of prediction made vs the total simulation time. In all instances, the prediction was made at the latest, half-way through the simulation. This implies that the algorithm is appropriate to diagnose proximity to instabilities in a power grid before any harm is done.

Lastly, it should be noted that while autocorrelation was used in both online/real-time (as Fixed Lag Autocorrelation) and offline/postmortem analyses (as Fixed Time Autocorrelation), the two usages were different in:

- their mode of procuring and processing input data (a running window of an incoming stream of data vs previously stored months/years worth of time series),

- the degrees of freedom allowed for its two parameter variables (which out of t and τ is allowed to be constant),

- their theoretically expected output data (autocorrelation is should decrease exponentially with respect to time lag τ but increase with time t if that the system is being progressively stressed with time)

Chapter 6

Summary and Conclusions

Offline/Postmortem Analysis

- Frequency time-series for months/years of data obtained from various real-world grids were converted into probability distribution function plots and autocorrelation decay plots ($c(\tau)$ vs τ plots).

- Visual inspection of the probability distribution function plots provided many insights into the presence of long-standing steady-state instabilities in the grid as well as the grid's resilience against any additional instability causing agents. Generally the PDFs of the more robust grids such as the RTE (France) and Continental European grids were mostly Gaussian except that they had heavier tails, whereas the smaller or island grids, such as the Mallorcan (Spain) grid had multiple peaks, skewed distributions and thus an overall visible deviation from Gaussianity which explains their higher susceptibility to steady-state deviations and thus a greater degree of vulnerability to grid failures.

- For most grids, the autocorrelation functions exponentially decayed with respect to time lag τ for smaller values of τ but certain grids showed significant deviation from the expected norm. For example the Continental European and UK grids showed a spike in autocorrelation decay function at time lags of every 15 minutes. This spike, which indicates an inherent instability causing agent in the grid systems, can be attributed to their 15 minute power trading intervals. Unlike the amount of transacted power which is suddenly varied every 15 minutes, the power grids, being dynamical systems cannot instantly adjust to the new power settings and thus the sudden imbalance of supply and demand leads to transients in the grid state variables.

- Autocorrelation decay curves of other grids (Nordic, Japan, US-Western Interconnection) initially decreased exponentially but later followed between a very slowly decaying or almost constant curve with respect to τ. This can be attributed to measurement error in the frequency detection.

- From the initial exponential decay of the curves, semi-log graphs were plotted and their inverse correlation times t_{corr}^{-1} were obtained. As per the Ornstein-Uhlenbeck Process this inverse correlation time can be likened to the damping constant α of the grids. As per our theoretical expectations, the bigger and more robust grids had higher values of α compared to the smaller, islanded grids.

Online/Real-time Analysis

- The IEEE 9 Bus System was progressively stressed in a time-domain simulation until 'bifurcation' was achieved [7]. In terms of implementation, 'bifurcation' was concluded to have taken place when the simulation solver could no longer converge to a solution without violating convergence thresholds. PSSE 34.3 simply calls out this occurrence as 'Network Not Converged'.

- The bus voltages were detrended with the help of a low pass filter, and their variance σ^2 as well as their Fixed Lag Autocorrelations (autocorrelations $c(t)$ with a fixed time lag $\tau = 1$ second) were computed over a running window.

- A new statistical parameter, called the Modified Kendall's τ Correlation Coefficient (MKTCC) was employed to check if the increase in the autocorrelations and variances was statistically significant. The reason for using a modified version of the normally used Kendall's τ Correlation Coefficient was to accommodate for the degree of certainty/confidence in predicting the correlation apart from the absolute value of correlation itself.

- Both autocorrelation and variance were found to be appropriate Early Warning Signs for indicators of an impending bifurcation, predicting the event early enough to make appropriate adjustments in the grid operation.

Chapter 7

Future Work

The grid analyzed for online/real-time analysis should be bigger, in order to demonstrate spatial variation in the early warning sign indicators for different buses/areas and for singling out areas which are more vulnerable to instabilities.

Despite the successful application of statistical analysis to detect symptoms of Critical Slowing Down in various phenomena [12], autocorrelation and variance are not certain indicators for the same, at least by themselves [27]. In order to tackle that, statistical parameters other than autocorrelation and variance can be investigated for their feasibility as Early Warning Signal indicators. Even for the same statistical indicators, changing the length of the running window, time lag τ, sampling rate etc. can have a significant effect on their effectiveness. Thus an 'optimal' set of parameters could be researched for, which may be different for different grids, but shouldn't vary for a particular grid once computed. On similar lines, grid state variables other than bus voltages, line current/MVAs, grid frequencies may be investigated.

References

[1] *Final report on the separation of the Continental Europe power system on 8 January 2021.* [Online; accessed 29. Jul. 2022]. July 2022. URL: https://www.entsoe.eu/news/2021/07/15/final-report-on-the-separation-of-the-continental-europe-power-system-on-8-january-2021.

[2] Benjamin Schäfer et al. "Non-Gaussian power grid frequency fluctuations characterized by Lévy-stable laws and superstatistics". In: *Nature Energy* 3.2 (Jan. 2018), pp. 119–126. ISSN: 2058-7546. DOI: 10.1038/s41560-017-0058-z. URL: http://dx.doi.org/10.1038/s41560-017-0058-z.

[3] William D. Rosehart and Claudio A. Caizares. "Bifurcation analysis of various power system models". In: *Int. J. Electr. Power Energy Syst.* 21.3 (Mar. 1999), pp. 171–182. ISSN: 0142-0615. DOI: 10.1016/S0142-0615(98)00037-4.

[4] Muhammad Adeen and Federico Milano. "On the Impact of Auto-Correlation of Stochastic Processes on the Transient Behavior of Power Systems". In: *IEEE Transactions on Power Systems* (2021), pp. 1–1. DOI: 10.1109/TPWRS.2021.3068038.

[5] Petr Vorobev et al. "Deadbands, Droop, and Inertia Impact on Power System Frequency Distribution". In: *IEEE Transactions on Power Systems* 34.4 (2019), pp. 3098–3108. DOI: 10.1109/TPWRS.2019.2895547.

[6] Francesca Madia Mele et al. "Impact of variability, uncertainty and frequency regulation on power system frequency distribution". In: *2016 Power Systems Computation Conference (PSCC)*. 2016, pp. 1–8. DOI: 10.1109/PSCC.2016.7540970.

[7] Eduardo Cotilla-Sanchez, Paul D. H. Hines, and Christopher M. Danforth. "Predicting Critical Transitions From Time Series Synchrophasor Data". In: *IEEE Transactions on Smart Grid* 3.4 (2012), pp. 1832–1840. DOI: 10.1109/TSG.2012.2213848.

[8] Goodarz Ghanavati, Paul D. H. Hines, and Taras I. Lakoba. "Identifying Useful Statistical Indicators of Proximity to Instability in Stochastic Power Systems". In: *IEEE Transactions on Power Systems* 31.2 (2016), pp. 1360–1368. DOI: 10.1109/TPWRS.2015.2412115.

[9] J. Nathan Kutz. "Advanced Differential Equations: Asymptotics & Perturbations". In: *arXiv* (Dec. 2020). DOI: `10.48550/arXiv.2012.14591`. eprint: `2012.14591`.

[10] Yushu Chen and Andrew Y. T. Leung. *Bifurcation and Chaos in Engineering.* London, England, UK: Springer. ISBN: 978-1-4471-1575-5. URL: `https://link.springer.com/book/10.1007/978-1-4471-1575-5`.

[11] Ronald R. Mohler. *Nonlinear Systems, Volume 1.* Upper Saddle River, NJ, USA: Prentice Hall, June 1990. ISBN: 978-0-13623489-0. URL: `https://www.goodreads.com/book/show/15197243-nonlinear-systems-volume-1`.

[12] Marten Scheffer et al. "Early-warning signals for critical transitions". In: *Nature* 461 (Sept. 2009), pp. 53–59. ISSN: 1476-4687. DOI: `10.1038/nature08227`.

[13] Leonardo Rydin Gorjão et al. "Open database analysis of scaling and spatio-temporal properties of power grid frequencies". In: *Nature Communications* 11.1 (Dec. 2020), p. 6362. ISSN: 2041-1723. DOI: `10.1038/s41467-020-19732-7`. URL: `https://doi.org/10.1038/s41467-020-19732-7`.

[14] Leonardo Rydin Gorjão. "Power-Grid-Frequency". In: *GitHub repository* (2020). URL: `https://github.com/LRydin/Power-Grid-Frequency`.

[15] Lisa Calearo, Andreas Thingvad, and Mattia Marinelli. "Grid Frequency Measurements of the Japanese (Tokyo area) Power System during 2017". In: (Oct. 2020). DOI: `10.11583/DTU.13142858.v1`. URL: `https://data.dtu.dk/articles/dataset/Grid_Frequency_Measurements_of_the_Japanese_Tokyo_area_Power_System_during_2017/13142858`.

[16] Andreas Thingvad, Lisa Calearo, and Mattia Marinelli. "Grid Frequency Measurements of the 50 Hz Japanese Power System during 2020". In: (Feb. 2021). DOI: `10.11583/DTU.14038910.v1`. URL: `https://data.dtu.dk/articles/dataset/Grid_Frequency_Measurements_of_the_50_Hz_Japanese_Power_System_during_2020/14038910`.

[17] Andreas Thingvad and Mattia Marinelli. "Grid Frequency Measurements of the Nordic Power System during 2018." In: (May 2020). DOI: `10.11583/DTU.12240260.v1`. URL: `https://data.dtu.dk/articles/dataset/Grid_Frequency_Measurements_of_the_Nordic_Power_System_during_2018_/12240260`.

[18] Andreas Thingvad and Mattia Marinelli. "Grid Frequency Measurements of the Nordic Power System during 2019". In: (Aug. 2020). DOI: 10.11583/DTU.12758573.v1. URL: https://data.dtu.dk/articles/dataset/Grid_Frequency_Measurements_of_the_Nordic_Power_System_during_2019/12758573.

[19] Andreas Thingvad and Mattia Marinelli. "Grid Frequency Measurements of the Continental European Power System during 2019". In: (Aug. 2020). DOI: 10.11583/DTU.12758429.v1. URL: https://data.dtu.dk/articles/dataset/Grid_Frequency_Measurements_of_the_Continental_European_Power_System_during_2019/12758429.

[20] Andreas Thingvad, Mattia Marinelli, and Lisa Calearo. "Grid Frequency Measurements of the Continental European Power System during 2020". In: (May 2021). DOI: 10.11583/DTU.14604927.v1. URL: https://data.dtu.dk/articles/dataset/Grid_Frequency_Measurements_of_the_Continental_European_Power_System_during_2020/14604927.

[21] Datopian. *ESO Data Portal: System Frequency - Dataset| National Grid Electricity System Operator.* [Online; accessed 28. Jul. 2022]. July 2022. URL: https://data.nationalgrideso.com/system/system-frequency-data.

[22] Christian Kuehn. "A mathematical framework for critical transitions: Bifurcations, fastslow systems and stochastic dynamics". In: *Physica D* 240.12 (June 2011), pp. 1020–1035. ISSN: 0167-2789. DOI: 10.1016/j.physd.2011.02.012.

[23] Luigi Vanfretti and Federico Milano. "Application of the PSAT, an Open Source Software, for Educational and Research Purposes". In: July 2007, pp. 1–7. DOI: 10.1109/PES.2007.385952.

[24] *Help - Python for PSSE help forum.* [Online; accessed 29. Jul. 2022]. July 2022. URL: https://psspy.org/psse-help-forum/help.

[25] Allen J. Wood and Bruce F. Wollenberg. *Power Generation, Operation, and Control.* Chichester, England, UK: WileyBlackwell, Mar. 1996. ISBN: 978-0-47158699-9. URL: https://www.amazon.in/Power-Generation-Operation-Control-Allen/dp/0471586994.

[26]   Peter E. Kloeden and Eckhard Platen. *Numerical Solution of Stochastic Differential Equations*. Berlin, Germany: Springer. ISBN: 978-3-662-12616-5. URL: `https://link.springer.com/book/10.1007/978-3-662-12616-5`.

[27]   Maarten C. Boerlijst, Thomas Oudman, and André M. de Roos. "Catastrophic Collapse Can Occur without Early Warning: Examples of Silent Catastrophes in Structured Ecological Models". In: *PLOS ONE* 8.4 (Apr. 2013), pp. 1–6. DOI: `10.1371/journal.pone.0062033`. URL: `https://doi.org/10.1371/journal.pone.0062033`.

[28]   Arthur Genthon. "The concept of velocity in the history of Brownian motion – From physics to mathematics and back". In: *arXiv* (June 2020). DOI: `10.1140/epjh/e2020-10009-8`. eprint: `2006.05399`.

[29]   *Lectures on Statistics*. [Online; accessed 4. Dec. 2022]. Dec. 2022. URL: `https://faculty.math.illinois.edu/~r-ash/Stat.html`.

Chapter A

Brownian Motion and the Ornstein-Uhlenbeck Process

Scientist Robert Brown quoted the term 'Brownian motion' to describe the random yet not chaotic motion of pollen grains suspended in water [28].

The Ornstein-Uhlenbeck Process (named in honour of Physicists Leonard Salomon Ornstein and George Eugene Uhlenbeck) is a special case of the Brownian Motion.
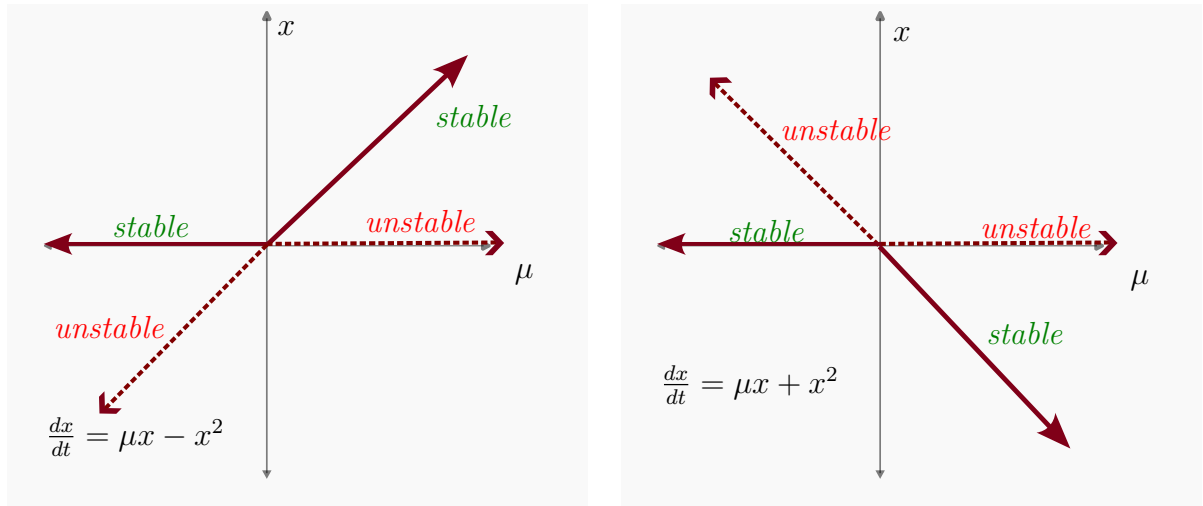
Chapter B

More Examples for Critical Bifurcation

Figure 22: Bifurcation diagrams for the normal forms of the Transcritical Bifurcation: $\frac{dx}{dt} = \mu x - x^2$ and $\frac{dx}{dt} = \mu x + x^2$
For $\mu \leq 0$, there are two fixed points (equilibrium points), $x = 0$ and $x = \mu$ (or $x = -\mu$), out of which one is stable and the other unstable. Upon reaching the critical 'tipping' point $\mu = 0$, the two fixed points or equilibrium solutions exchange their stabilities. The tipping point $\mu = 0$ is a bifurcation point.

Chapter C

A Comparison of select Correlation Coefficients

Pearson's Correlation Coefficient

Pearson's Correlation Coefficient, often denoted using the parameter ρ, is one of the go-to methods for computing the degree of correspondence between two datasets or time-series, etc. The value of ρ varies between positive and negative unity, i.e. $-1 \leq \rho \leq +1$, where the more the value is skewed towards either extreme end, the more correlated the two datasets or time-series are. The sign determines if the correlation is positive or negative. A value of ρ closer to 0 implies little to no correlation between the two variables.

Table 3 gives a quick overview of this correlation coefficient.

Spearman's Ranked Correlation Coefficient

Kendall's Correlation Coefficient

Modified Kendall's Correlation Coefficient

Table 3: Interpretation of different values of the Pearson's ρ Correlation Coefficient.

Pearson's Correlation Coefficient ρ	Interpretation	Examples of two variables specific to Power Systems following the relationship
$\rho \in (0,1]$	A positive value of the correlation coefficient implies that both the variables change in the same 'direction'.	Population of a city vs Daily Power Demand Transmission Line Length vs Line Losses
$\rho \approx 0$	A near zero value of the correlation coefficient implies that both the variables are uncorrelated. In some special cases, such as the case of jointly Gaussian variables, a zero correlation implies the independence of the two variables. [29]	Nominal Frequency of Grid vs Wattage of end-user electronics Nominal Frequency vs Setting of a Distance Relay
$\rho \in (-1,0)$	A negative value of the correlation coefficient implies that the variables change in opposite 'directions'.	Maximum Loadability of a Line vs Line Reactance Bus Voltage vs Line current flowing into that Bus